Neutron Resonance Spectroscopy. IV. As and Br†

J. B. GARG, W. W. HAVENS, JR., AND J. RAINWATER
Columbia University, New York, New York

(Received 25 May 1964)

The Columbia neutron velocity spectrometer with a 200-m flight path was used for total-cross-section measurements using several transmission sample thicknesses each of natural As(100% As^{75}, $I=3/2$) and Br (~50% each Br^{79} and Br^{81}, both $I=\frac{3}{2}$). The values of $g\Gamma_n^0$ for 136 levels in As (to 10 keV) and 157 levels in Br (to 4 keV) have been determined. Γ_γ and J values were also determined for many of the stronger levels. The $l=0$ strength function S_0 was found to be $(1.70\pm0.30)\times10^{-4}$ for As and $(1.20\pm0.18)\times10^{-4}$ for Br. The S_0 values are averaged over both spin states and, in the case of Br, S_0 is also averaged over the two isotopes. There were many more levels with very small values of $g\Gamma_n^0$ for both As and Br than expected from the Porter-Thomas distribution for a single channel and a single population. The experimental value of $\langle D\rangle$ for all of the observed levels is 71 eV for As and 25.5 eV for Br. A best Porter-Thomas fit to the stronger levels alone, gives $\langle D\rangle=87$ eV for As and 36.5 eV for Br. Assuming an approximate theoretical value of (−0.25) for the correlation coefficient between adjacent level spacings, 8 of the observed very weak As levels and 17 of the Br levels were selected as most likely to be unreliable, or due to $l=1$. Hence 128 levels for As and 140 levels for Br were used for most of the tests of statistical distribution parameters. This gives $\langle D\rangle=75$ eV for As and 28.4 eV for Br. A considerable number of the weaker levels for each element are probably p-wave levels. Statistical analyses are given of the distributions for $g\Gamma_n^0$, D^0, D^1, and various correlation coefficients involving the $g\Gamma_n^0$ values and the spacings. D^0 is the nearest-neighbor level spacing, and D^1 is the next-nearest-neighbor level spacing. Comparisons are made with the predictions of various theories.

1. INTRODUCTION

THIS is the fourth in a series[1–3] of papers reporting results using the Columbia University Nevis synchrocyclotron for time-of-flight neutron spectroscopy. It is the second paper reporting the results of total neutron cross-section measurements using a 200-m flight path, having 0.5-nsec/m resolution for $E\gg1$ keV. The spectrometer system has been described elsewhere.[4] Resonance parameters are determined using area analysis, as described in the preceding paper[3] of this series for the case of a single isotope with $I=0$. Modifications for the case $I\neq0$ are discussed in Ref. 2. A feature of present measurements is the determination of level parameters for a large numer of levels for neutron energies from ~100 eV to a few keV for each element. The precision is greatly improved for the evaluation of the various statistical parameters which have previously been determined using only a small number of the lowest energy resonances of these elements. We require relatively large samples. This implies that our measurements are largely restricted to samples having the natural isotopic abundances for the elements studied.

This paper presents the results of total cross-section measurements using several sample thicknesses each of As (100% As^{75}, $Z=33$, $I=\frac{3}{2}$) and Br (about 50% each of Br^{79} and Br^{81}, $Z=35$, both $I=\frac{3}{2}$). The measurements on As covered the energy region from 200 to 10 000 eV. The measurements on Br covered the energy region from 100 to 4000 eV. Earlier measurements[5–7] for these elements were made using considerably poorer neutron energy resolution, so only a few levels could be observed in each case. In the present measurements we have obtained level parameters for 136 levels in As and 157 levels in Br.

Earlier (1959–1960) results for As and Br obtained in this laboratory using a 35-m flight path and self-indication techniques have previously been presented at meetings[7] only. We include here portions of the earlier unpublished results (mainly for the lower energy levels) which supplement the present 200-m flight path measurements to give a more complete experimental evaluation of the level systematics. The experimental count versus energy data, and its analysis, was similar to that of Ref. 2.

One of the interesting reasons for obtaining a precise measurement of the s-wave strength function of these nuclei relates to the suggestion[5] that the $l=0$ strength function for $40<A<90$ shows a second smaller maximum near $A\sim80$, with a weak minimum near $A\sim70$ separating it from the main maximum near $A\sim50$. A detailed examination of the resonance parameter de-

† Work supported in part by the U. S. Atomic Energy Commission.

[1] J. L. Rosen, J. S. Desjardins, J. Rainwater, and W. W. Havens, Jr., Phys. Rev. **118**, 687 (1960).

[2] J. S. Desjardins, J. L. Rosen, W. W. Havens, Jr., and J. Rainwater, Phys. Rev. **120**, 2114 (1960).

[3] J. B. Garg, J. Rainwater, J. S. Petersen, W. W. Havens, Jr., Phys. Rev. **134**, B985 (1964).

[4] J. Rainwater, W. W. Havens, Jr., and J. B. Garg, Rev. Sci. Instr. **35**, 263 (1964).

[5] R. E. Coté, L. M. Bollinger, and J. M. Leblanc, Phys. Rev. **111**, 288 (1958). J. M. Leblanc, R. E. Coté, and L. M. Bollinger, Nucl. Phys. **14**, 120 (1959). Figure 3 of this paper illustrates the shape of the proposed double peak in the s-wave strength function.

[6] H. Marshak and H. Newson, Phys. Rev. **106**, 110 (1957).

[7] J. Rosen, S. Desjardins, W. W. Havens, Jr., and L. J. Rainwater, Bull. Am. Phys. Soc. 4, 271 (1959). S. Desjardins, W. W. Havens, Jr., J. Rainwater, J. L. Rosen, *ibid.* **5**, 295 (1960).

The 1959 measurements for As used a 35-m flight path and self-indication detection. The measurements for the 47.0- and 92.2-eV levels used detector and transmission sample thicknesses having $(1/n)=177$ and 111 b/atom, respectively. Only the results for these two levels are included in the present paper.

The 1960 self-indication 35-m flight path measurements for Br used $PbBr_2$ samples. The "D" sample had $(1/n)=336$ b/atom of Br. Two transmission were used having $(1/n)=336$ and 112 b/atom of Br, respectively. The experimental data curves and the analysis methods were similar to those in Ref. 2.

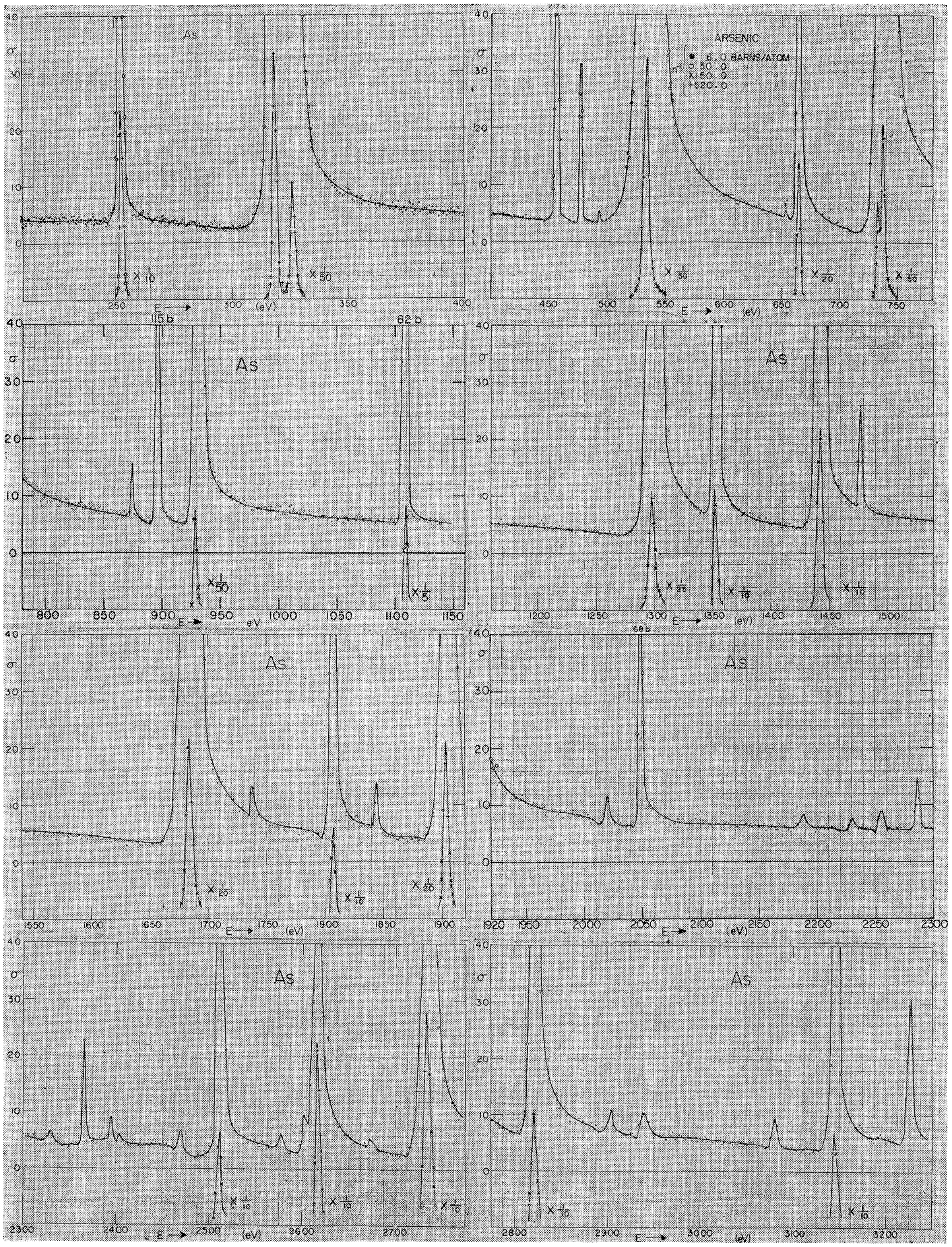
As
ARSENIC
6.0 BARNS/ATOM
30.0
150.0
520.0
σ
E →
(eV)
X 1/10
X 1/50
X 1/20
X 1/5
X 1/25
115 b
82 b
68 b

(a)

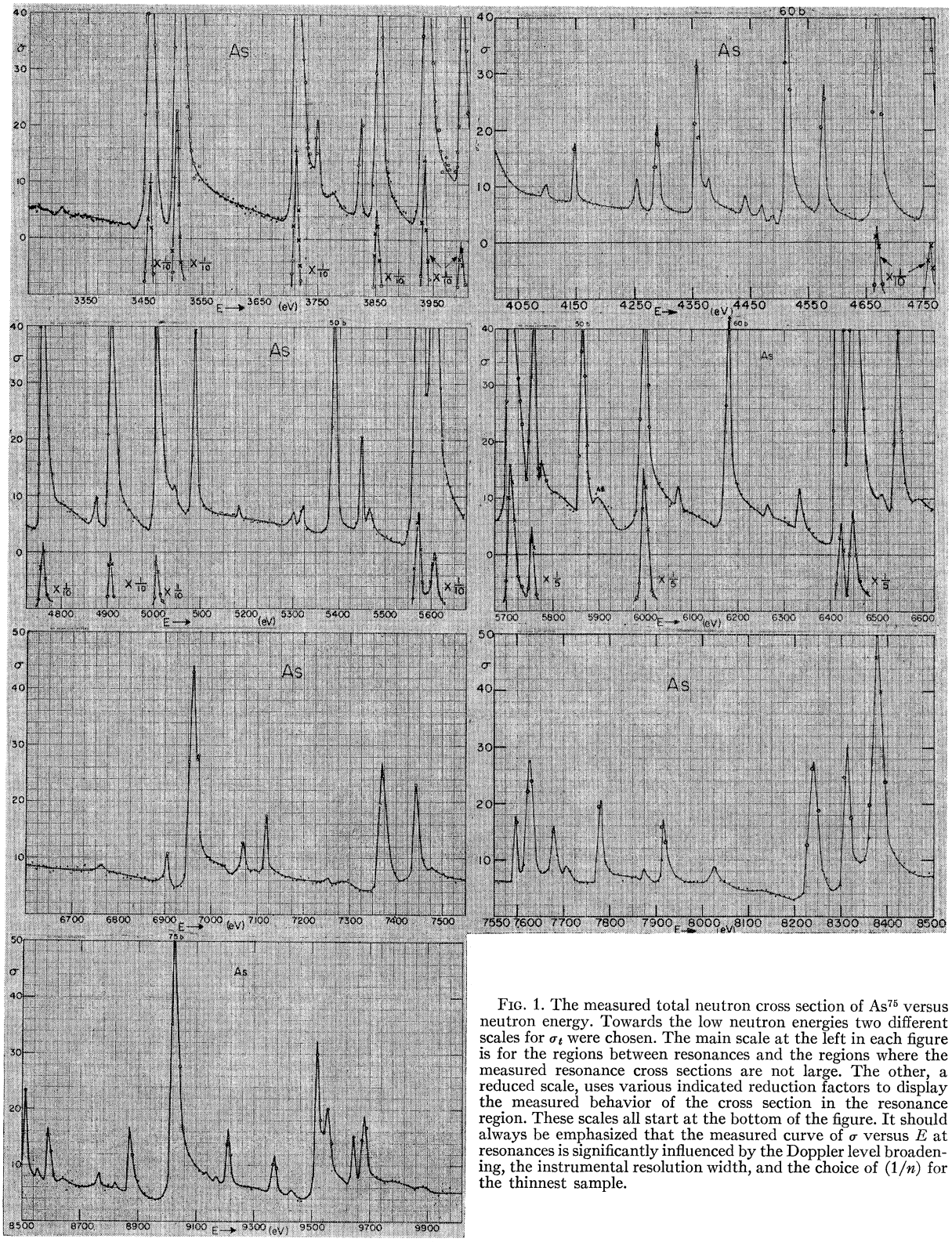

FIG. 1. The measured total neutron cross section of As^{75} versus neutron energy. Towards the low neutron energies two different scales for σ_t were chosen. The main scale at the left in each figure is for the regions between resonances and the regions where the measured resonance cross sections are not large. The other, a reduced scale, uses various indicated reduction factors to display the measured behavior of the cross section in the resonance region. These scales all start at the bottom of the figure. It should always be emphasized that the measured curve of σ versus E at resonances is significantly influenced by the Doppler level broadening, the instrumental resolution width, and the choice of $(1/n)$ for the thinnest sample.

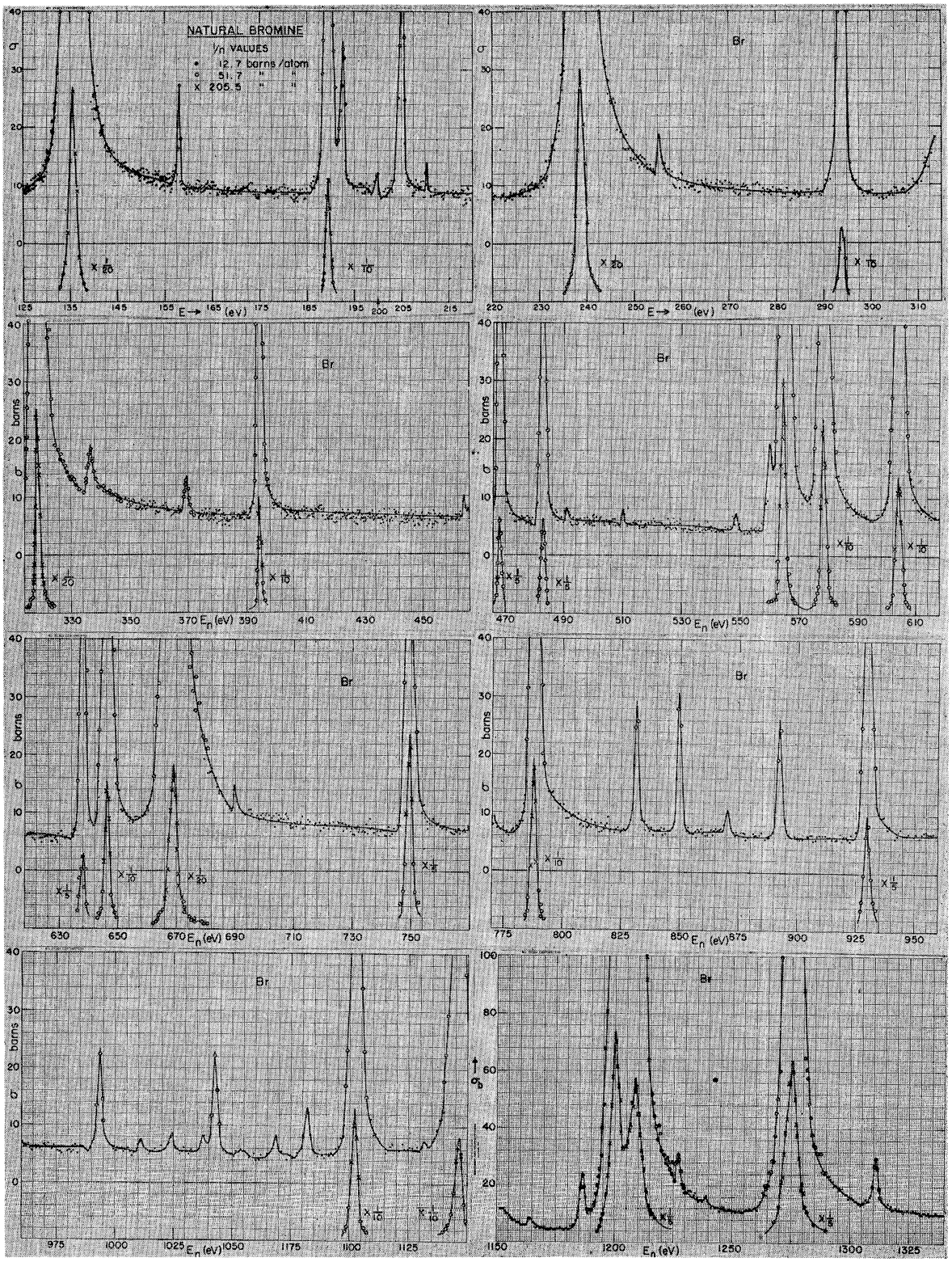
NATURAL BROMINE
1/n VALUES
• 12.7 barns/atom
○ 51.7 " "
X 205.5 " "
Br
barns
E → (eV)
E_n (eV)

(a)

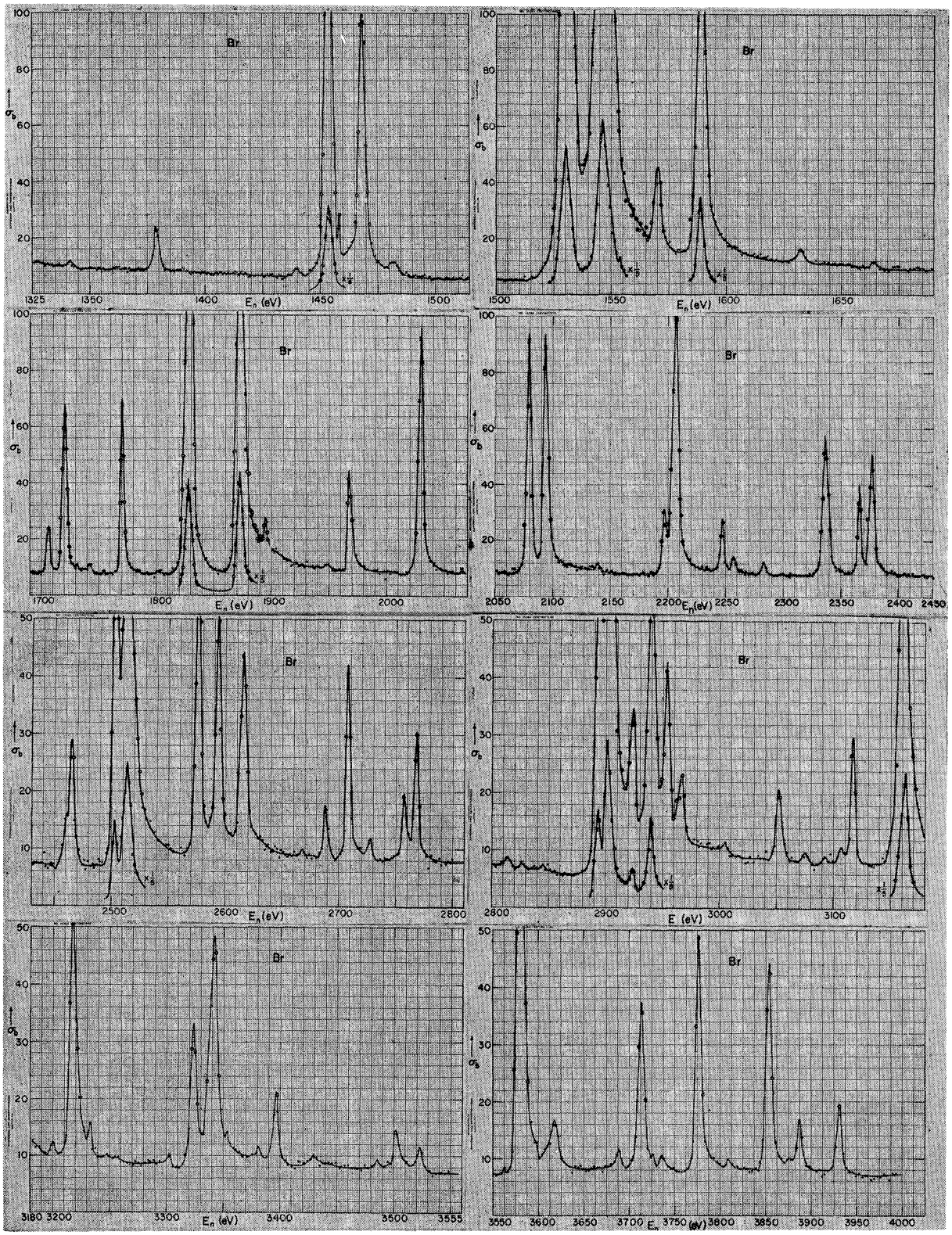

(b)

FIG. 2. The "measured" cross section of Br versus neutron energy. Values are for the natural element which has about 50% abundance each of Br^{79} and Br^{81}. The "measured" peak cross sections are limited experimentally to values which are not large compared to the value $(1/n) = 205.5$ b/atom of the thinnest sample, so they may be small compared with the true Doppler-broadened peak cross section.

TABLE I. Resonance parameters for the levels in arsenic. The last column lists the value of J favored by the analysis. The results for the first two levels are from the 35-m measurements.[7] The levels indicated by * are considered most apt to be spurious, or due to $l=1$ interactions. They are omitted in most of the statistical analysis of the data. The absolute level uncertainty ΔE_0 is larger than the uncertainty in the relative level positions. Since $g=\frac{3}{8}$ or $\frac{5}{8}$ for $J=1$ or 2, respectively $2g\Gamma_n^0$ is roughly the same as Γ_n^0. A choice $\Gamma_\gamma=300$ meV was assumed in most cases to obtain a best choice for $2g\Gamma_n^0$.

E_0 (eV)	ΔE_0 (eV)	$2g\Gamma_n^0$ (meV)	$\Delta 2g\Gamma_n^0$ (meV)	Preferred J
47.0	0.1	6.5	0.4	
92.2	0.2	1.6	0.2	
252.7	0.3	3.70	0.3	···
318.6	0.3	33	3	2
326.7	0.3	24	1	1
455.5	0.3	1.64	0.2	···
476.9	0.3	0.44	0.04	···
*493.3	0.3	0.06	0.02	···
533.4	0.6	140	12	2
664.9	0.5	11.6	0.8	2
733.3	0.5	34	2	1
737.4	0.5	96	4	2
*874.6	0.6	0.20	0.04	···
895.5	0.7	5.6	1.0	···
929.4	0.8	40	4	2
1110.4	1.0	3.6	0.6	···
1299.0	1.0	70	6	2
1353	1.5	15	2	1
1442.6	1.5	26	4	2
1479.3	1.5	1.3	0.4	···
1683.6	1.5	92	4	2
1739.0	2.0	0.30	0.08	···
1807.2	1.0	12.4	1.0	···
1845.6	1.0	0.4	0.06	···
1903.9	1.0	90	6	2
2021.1	1.0	0.4	0.08	···
2049.2	1.0	5.7	1.0	···
2190	1.5	0.24	0.08	···
*2232	1.5	0.12	0.04	···
2256	1.5	0.34	0.06	···
2288	1.5	0.50	0.10	···
2330	1.5	0.22	0.04	···
2365	1.5	1.80	0.10	···
2395	1.5	0.36	0.06	···
*2403	1.5	0.10	0.04	···
2470	1.5	0.30	0.10	···
2511	1.5	21	1	1
2577	1.5	0.30	0.08	···
2616	1.5	60	8	2
2673	2	0.22	0.08	···
2733	2	84	10	2
2821	2	48	4	(1)
2902	2	0.56	0.08	···
2939	2	0.90	0.20	···
3081	2.5	0.96	0.2	···
3144	2.5	34	4	···
3227	2.5	7.4	1.4	···
3306	2.5	0.26	0.1	···
3459	3	58	6	2
3505	3	120	16	2
3712	3	80	10	2
3749	3	1.6	0.4	···
*3777	3	0.18	0.08	···
3822	3	3.6	0.4	1
3852	3.5	50	6	(2)
3933	3.5	84	10	2
3998	3.5	34	4	1
4096	3.5	0.6	0.2	···
4146	4	2.6	0.8	···
4253	4	1.3	0.3	···
4289	4	5.0	0.8	···
4358	4	12	2	···
4378	4	0.30	0.10	···
4442	4	0.9	0.2	···
4470	4	0.54	0.20	···
*4488	4	0.18	0.10	···
4514	4	22	4	···
4576	4	7.6	1.4	···
4669	4	60	6	···
4761	4.5	48	6	···
4875	4.5	0.8	0.2	···
4905	4.5	52	8	···
5006	5	54	8	···
5043	5	0.2	0.2	···
5090	5	20	4	···
5183	5	0.5	0.2	···
5303	5	0.6	0.2	···
5324	5	0.7	0.2	···
5387	5.5	23	4	···
5446	5.5	8	2	···
5466	5.5	0.5	0.2	···
5573	5.5	124	10	···
5610	5.5	50	10	···
5709	6	100	20	···
5755	6	36	4	···
5775	6	0.5	0.2	···
5863	6	30	4	···
5998	6	106	20	···
6070	6.5	1.0	0.4	···
6178	6.5	42	8	···
6265	6.5	0.6	0.2	···
6336	6.5	5.0	1.0	···
6423	7	60	8	···
6450	7	64	8	···
*6506	7	0.2	0.2	···
6549	7	26	6	···
6593	7	0.6	0.2	···
6765	7	0.9	0.4	···
6904	7.5	2.6	1.0	···
6959	7.5	64	8	···
7071	7.5	5	1	···
7121	7.5	2	2	···
7254	7.5	0.3	0.1	···
7297	8	0.2	0.1	···
7370	8	30	6	···
7443	8	20	4	···
7479	8	0.2	0.1	···
7596	9	7.0	1.6	···
7627	9	20	4	···
7680	9	6	1.2	···
7706	9	2.0	1.0	···
7778	9	15	3	···
7875	10	1.4	0.3	···
7920	10	7.4	1.0	···
8026	10	3.0	1.0	···
8240	10	38	8	···
8315	10	30	6	···
8380	10	64	10	···
*8449	10	0.2	0.2	···
8508	10	24	4	···
8556	11	2.4	1.0	···
8590	11	9	2	···
8650	11	0.8	0.4	···
8766	11	3	1	···
8823	11	0.76	0.4	···
8880	11	15	4	···
9030	11	114	20	···
9135	12	0.6	0.6	···
9173	12	0.8	0.4	···
9215	12	13	3	···
9375	12	8	2	···
9430	12	2	1	···
9520	13	44	10	···
9557	13	24	6	···
9647	13	6	2	···
9686	13	15	4	···

TABLE II. Resonance parameters of levels in natural bromine. The parameter $4a\Gamma_n^0 \approx \Gamma_n^0$, since $a=0.5$ for both Br^{79} and Br^{81} and $g=\frac{3}{8}$ or $\frac{5}{8}$ for levels having $J=1$ or 2, respectively. Values from the 35-m measurements[7] are indicated by *C* in the E_0 column, while an *A* indicates results from Ref. 5. See the caption for Table I for further comments which also apply to this table.

E_0 (eV)	ΔE_0 (eV)	$4ag\Gamma_n^0$ (meV)	$\Delta 4ag\Gamma_n^0$ (meV)
35.8 *C*	0.1	9.0	0.6
A		9.4	0.7
53.7 *C*	0.1	3.7	0.2
A		3.1	0.3
101.01	0.08	20	1
C		18.8	0.9
135.50	0.10	28	2.2
C		28	2
157.98	0.10	0.07	0.01
189.52	0.15	4.4	0.4
C		5.1	0.4
192.72	0.15	0.36	0.12
C		0.25	0.03
205.00	0.15	0.8	0.1
C		1.05	0.1
*210.4	0.20	0.044	0.008
238.5	0.20	44	4
C		49	4
255.2	0.20	0.12	0.04
C		0.12	0.03
293.7	0.25	4.2	0.4
C		4.3	0.4
318.5	0.30	40	4
C		43	4.3
336.8	0.15	0.10	0.02
C		0.16	0.03
369.1	0.20	0.14	0.02
C		0.21	0.04
394.5	0.2	6.8	0.8
C		7.1	1.1
464.3	0.3	0.06	0.02
467.9	0.3	2.6	0.4
C		4.6	0.7
483.2	0.3	3.0	0.4
C		5.0	0.7
490.5	0.3	0.06	0.02
*510.2	0.3	0.08	0.02
*548.8	0.3	0.04	0.02
560.3	0.4	0.64	0.2
564.8	0.4	24	2
C		21	5
578.6	0.4	18	2
C		18	4
604.2	0.4	15.2	0.8
C		17	3
637.8	0.4	3.8	0.4
C	0.4	6.9	1
646.2	0.5	16.8	2
C		21	3
668.8	0.5	70	8
C		54	18
689.4	0.5	0.04	0.02
749.3	0.55	12	1.2
C		20	7
771.0	0.6	0.12	0.04
788.0	0.6	27.2	2
C		28	14
831.2	0.65	1.9	0.2
C		3.0	0.4
849.5	0.65	1.7	0.2
C		2.2	0.3
870.0	0.7	0.28	0.08
C		0.44	0.07
892.3	0.7	1.7	0.2
C		1.3	1
930.8	0.8	12	1.2
C		11.8	2.6
993.5	0.85	1.4	0.2
1011.0	0.9	0.16	0.08
*1024.0	0.9	0.24	0.12
1037.7	0.9	0.12	0.04
1042.5	0.9	1.5	0.2
1068.5	0.95	0.20	0.08
1082.0	1.0	0.72	0.2
1102.0	1.0	34	4
1146.5	1.1	33	4
1164.5	1.1	0.12	0.08
1187.0	1.1	1.24	0.2
1200.0	0.55	54	16
1208.5	0.6	60	12
*1227	0.6	1.36	0.16
*1239	0.6	0.04	0.02
1275	0.6	80	16
1311	0.7	1.6	0.2
1342	0.7	0.08	0.04
1378.5	0.7	1.6	0.2
1440.5	0.7	0.28	0.08
1454	0.8	23	2
1468	0.8	17	2
*1482	0.8	0.24	0.08
1530	0.8	72	12
1546.5	0.8	116	20
1570	0.9	4.0	0.8
1589	0.9	32	3
1632	0.9	0.6	0.2
1664	0.9	0.28	0.08
1674	1.0	0.12	0.04
1706.5	1.0	2.8	0.3
1720	1.0	12.8	2
1743	1.0	0.24	0.12
*1755	1.0	0.08	0.08
1770	1.0	12.4	2
*1802	1.1	0.08	0.08
1828	1.1	60	8
1872.5	1.1	70	8
1895	1.1	1.2	0.4
*1904	1.2	0.08	0.08
1948	1.2	0.20	0.08
1967	1.2	8.8	1.6
2030	1.3	23	3
2065	1.3	0.08	0.08
2079.5	1.3	20	2
2093.5	1.3	23	2
2139.5	1.4	0.35	0.2
2196	1.4	4.4	2
2206	1.4	34	4
*2235	1.5	0.08	0.08
2247.5	1.5	3.3	0.4
2257	1.5	0.8	0.2
2283	1.5	1.1	0.2
2336	1.6	15	2
2366	1.6	6.8	1.2
2377	1.6	10	2
2395	1.6	0.2	0.1
2461	1.7	2.0	0.8
2465	1.7	6	2
2503	1.7	18	4
2514	1.8	58	12
*2535	1.8	0.2	0.2
2576	1.8	16	2
2593	1.8	14	2
2616	1.9	13	2
*2643	1.9	0.16	0.08
2668	1.9	0.16	0.08
2688	1.9	2.4	0.4
2707	2.0	12	2
2727	2.0	1.08	0.2
2757	2.0	2.5	0.4
2768	2.0	6.4	1.2
2813	2.1	0.28	0.12
2826	2.1	0.12	0.04
*2846	2.1	0.12	0.04

TABLE II (*continued*)

E_0 (eV)	ΔE_0 (eV)	$4ag\Gamma_n^0$ (meV)	$\Delta 4ag\Gamma_n^0$ (meV)
2893	2.1	24	8
2901	2.2	80	20
2924	2.2	5.4	1.2
2940	2.2	22	4
2954	2.2	8	4
2967	2.2	4	2
3005	2.3	0.2	0.08
*3042	2.3	0.2	0.2
3053	2.3	2.8	1.2
3076	2.3	0.5	0.16
3093	2.4	0.3	0.1
3107	2.4	0.3	0.1
3117	2.4	5.6	0.8
3162	2.5	60	8
3200	2.5	0.5	0.2
3218	2.5	33	6
3232	2.5	1.1	0.2
3247	2.6	0.20	0.08
3303	2.6	0.24	0.12
3323	2.6	10.4	1.6
3341	2.7	26	4
*3354	2.7	0.2	0.2
3381	2.7	0.36	0.2
3396	2.7	4	0.8
3430	2.8	0.7	0.3
3486	2.8	0.20	0.08
3503	2.8	2.0	0.4
3523	2.8	1.0	0.4
3563	2.9	0.2	0.08
3582	2.9	56	8
3597	3.0	0.4	0.2
3610	3.0	2.0	1.2
3617	3.0	5	2
3662	3.1	0.20	0.12
3688	3.1	0.96	0.4
3713	3.1	15	4
3726	3.2	0.2	0.1
3737	3.2	0.6	0.2
3775	3.2	25	5
*3809	3.3	0.5	0.2
3853	3.3	25	5
3874	3.3	0.2	0.1
3888	3.4	5	1
3931	3.4	7	2
...	...	...	...
...	...	...	...
...	...	...	...

terminations which form the basis of the plot of the s-wave strength function S_0 versus A suggests that there is a rather large uncertainty in the proper form for the curve.

II. EXPERIMENTAL DETAILS AND LEVEL PARAMETER ANALYSIS

A. Arsenic

Sample thicknesses of $1/n=6.0$, 30.0, 150, and 520 b/atom of arsenic powder were used. The material, including a small amount of sulfur as binder, was packed in containers using thin Al on the surfaces traversed by the neutrons. Detection channel widths of 0.2 μsec were used in the energy region from 200 eV to 1800 eV, corresponding to an energy resolution $\Delta E\approx 1$ eV at 1000 eV. This compares with $2\Delta=2.5$ eV, where Δ is the Doppler level broadening half-width.[4] Detection channel widths of 0.1 μsec were used in the energy interval from 1800 to 10 000 eV, corresponding to $\sim$0.5 nsec/m. At 10 keV the resolution width is $\sim$15-eV instrumental energy resolution, while $2\Delta=7.3$ eV. These values are small compared with our observed average level spacing of 75 eV for arsenic.

The "measured" total cross section versus energy curves for As are shown in Fig. 1. The cross section values between resonances were determined from measurements on the thickest sample. The measured cross section in the region of the resonances is distorted by the effects of the experimental energy resolution, the Doppler broadening and the choice of the sample $1/n$ values. These effects have been discussed in a preceding paper.[3]

The method of level parameter analysis is similar to that described[3] for Th^{232} and U^{238}. In order to take the spin into account, the theoretical resonance cross-section terms must be multiplied by the spin weight factor $g=\frac{3}{8}$ or $\frac{5}{8}$. Unless otherwise indicated, a value $g=\frac{1}{2}$ was assumed in the analysis. In certain favorable circumstances an angular momentum assignment $J=1$ or 2, of the compound nuclear state is given. For these resonances the alternate choice of J led to an unreasonable Γ_γ, while an assumed $\Gamma_\gamma=300$ meV gave internal consistency for the results using different sample thicknesses. The results are given in Table I. The values $2g\Gamma_n^0$ are approximately equal to Γ_n^0.

In certain cases, for both As and Br, the analysis also yielded values of Γ with sufficiently small uncertainty, independent of an assumed value for g. Table III lists these cases and shows the implied value of Γ_n and Γ_γ for each choice of J. Where one J value gives $\Gamma_\gamma\approx 300$ meV, and the other does not, that J value is favored which gave $\Gamma_\gamma\approx 300$ meV.

The 35-m measurements[7] gave $E_0=(47.0\pm 0.1)$ eV, and $g\Gamma_n\Gamma=(0.00785\pm 0.0005)$ $(\text{eV})^2$ for the first As level. The result for $g\Gamma_n\Gamma$ was insensitive to the choice of Γ_γ. The next level was found to have $E_0=(92.2\pm 0.2)$ eV. In this case the "D" and the "$D+T$" information yielded a solution favoring $\Gamma=324$ meV and $g\Gamma_n=7.75$ meV.

B. Bromine

Three sample thicknesses were used having $1/n=12.7$, 51.7, and 205.5 b/atom of natural Br ($\sim$50% each Br^{79} and Br^{81}) in the form of CBr_4 in containers employing thin Al windows. The effect of the constant carbon cross section was subtracted during the data processing. The measurements were performed in three energy intervals: 100 to 300 eV, 300 to 1100 eV, and 1100 to 4000 eV using 0.4-, 0.2-, and 0.1-μsec detection channel widths, respectively. At the highest energy the experimental energy resolution width was about 5 eV, at which energy 2Δ was also about 5 eV. At lower energies the Doppler width dominates. The $1/n$ value of the thinnest sample was much smaller than the Doppler-broadened peak cross sections for the strong reson-

TABLE III. Resonance parameters for levels in arsenic and bromine for which there is additional information concerning Γ, Γ_γ, Γ_n, or J. The italicized values for the present measurements indicate the choice that gives the favored J value. These results supplement those of Tables I and II. *C* results for the 35 m self-indication measurements.[7] *A* values from Refs. 5 (which also provides all Br isotope identification). The Γ_γ values for *C* and *B*, together with their stated uncertainties, apply for either choice of J. The symbol * means that $\Gamma_\gamma = 300$ meV was assumed.

E_0 (eV)		A	J	Γ (meV)	$\Delta\Gamma$	Γ_n(meV) $J=1$	Γ_n(meV) $J=2$	Γ_γ (meV) $J=1$	Γ_γ (meV) $J=2$
				Arsenic					
47.0	*C*	75	...	...	...	*59	*37	...	...
	A		...	336	32	52	31	285	305
92.2	*C*		...	324	50	20.7	12.5	303	311
	A		...	286	89	21	12	265	274
252.7				320	30	78	47	242	273
	A			300	150	93	56		
318.6			2	650	50	780	*470*	neg	*180*
326.7			1	980	50	*576*	346	*404*	634
455.5				370	30	47	28	323	342
476.9				350	50	13	8	337	342
533.4			2	2600	300	4350	*2590*	neg	*10*
664.9			2	555	50	398	*238*	152	*312*
733.3			1	*1530	100	*1230*	739	(300)	*
737.4			2	*2400	100	3070	*2080*	*	(300)
895.5				450	50	223	*134*	227	*316*
929.4			2	1150	150	1630	*978*	neg	*122*
1010.4				500	50	*161*	97	*339*	403
1299.0			2	2400	250	3360	*2020*	neg	*380*
1353			1	980	100	*732*	440	*248*	540
1442.6			2	1700	150	2700	*1390*	neg	*310*
1683.6			2	3500	300	5020	*3010*	neg	*490*
1807.2				850	100	706	422	94	428
1903.9			2	3000	500	5230	*3140*	neg	*~0*
				Bromine					
35.8	*C*		...	...	...	70	43	(280±	40)
	A	79	...	...	...	75	45	(310±	30)
53.7	*C*		...	...	...	36	21	(423±	40)
	A	79	...	...	...	31	18	(430±	70)
101.01			...	...	...	267	160		
	C		2	...	...	250	150	(252±	25)
	A	81	...	...	...	270	160	(210±	120)
135.50			(2)	600	50	427	*260*	173	*339*
	C		(1)	...	...	437	253	(344±	40)
	A	81	...	...	...	440	260	(370±	140)
189.5			...	400	50	80	48	320	352
	C		1	...	...	93	56	(450±	90)
	A	79	...	...	...	104	62	(410±	140)
238.5			(2)	850	50	906	544	neg	*306*
	C		...	...	...	1015	610	...	...
	A	79	...	...	...	1110	660	(460±	30)
293.7			(2)	300	50	96	58	204	*242*
	C		...	...	...	97	59	...	...
	A	79	...	...	...	109	66	...	...
318.5	*C*		1	...	...	1030	620	(400±	120)
394.5		79	(2)	380	80	180	108	200	*272*
	A		...	...	...	187	112	(368±	74)
468.0				350	70	82	50	268	301
	C			...	...	133	80	...	...
483.2				370	70	88	53	282	317
	C			...	...	147	88	(270±	50)
564			(2)	750	50	760	466	neg	*284*
578.6			(2)	660	60	586	346	74	*314*
	C		...		...	578	350	(350±	60)
604.2			...	750	100	500	297	250	457
	C		...			560	337	...	...
646.2			(2)	550	100	570	342	neg	*208*
	C					720	430	(380±	75)

ances toward the low-energy end of the spectrum.

The "measured" total cross section versus energy curves for Br are shown in Fig. 2. The same remarks apply for these curves as in Fig. 1. The cross section given in the figure is for the *element*. The results for the level parameters obtained are given in Table II. Both isotopes have $I=\frac{3}{2}$ and essentially equal abundance so $a=0.5$ for each isotope. Since the g factor is $\frac{3}{8}$ or $\frac{5}{8}$ for $J=1$ or 2, respectively, the tabulated quantity $4ag\Gamma_n^0$ is approximately equal to Γ_n^0. Since only the g

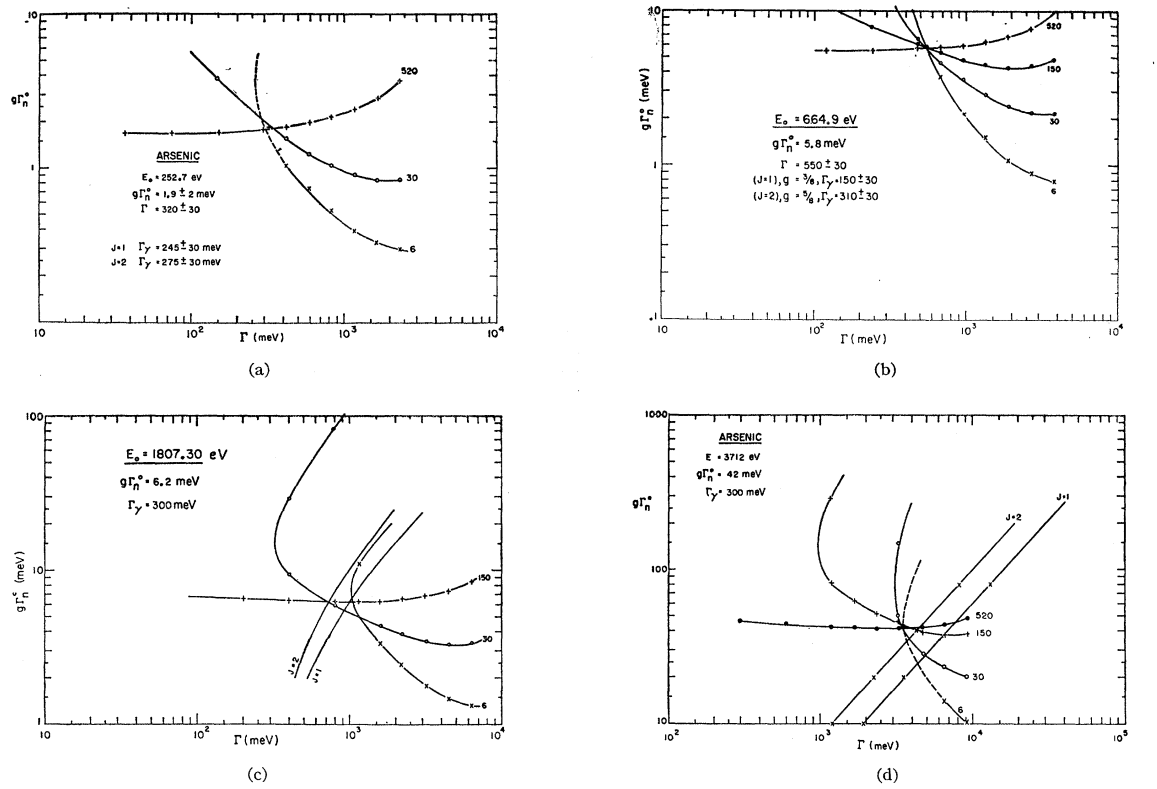

FIG. 3. Examples of the level parameter analysis for four levels of arsenic. For each level there is one curve each showing the implied relationship between the values of $g\Gamma_n^0$ and Γ for each transmission sample. The curves are labeled by the sample $1/n$ value. For the analysis techniques see Refs. 2 and 3. Two of the level curves show the implied relation between $g\Gamma_n^0$ and Γ if Γ_γ is chosen to be 300 meV. Note that $\Gamma \equiv \Gamma_\gamma + \Gamma_n$.

value (and the isotopic assignment) of a resonance is unknown, the analysis problem is similar to that for As, except for the smaller average level spacing and greater fraction of relatively small level spacings. After a detailed study of the analysis plots for each resonance, we decided that in most cases there was inadequate accuracy to evaluate the compound nuclear J value, so the analysis determines $g\Gamma_n^0$. A value of $\Gamma_\gamma = 300$ meV was assumed unless a value of Γ_γ for the level is shown in Table III. The thin-sample analysis gives $g\Gamma_n^0$ values which are reasonably insensitive to the exact choice of Γ_γ or of g. Table III lists the cases in the present measurements where $g\Gamma_n^0$ and Γ can both be determined independently, so the J-dependent choices for Γ_n and Γ_γ can be listed. The J value giving $\Gamma_\gamma \approx 300$ meV is favored.

Table II also lists some of the values of $4ag\Gamma_n^0$ from our previously unpublished results[7] for Br (using a 35-m flight path and self-indication techniques). The 35- and 200-m results are completely independent, since the earlier results were not re-examined until the final values for the 200-m measurement level parameters had been obtained. The general agreement is excellent in most cases. The self-indication measurements also gave values of Γ_γ for a number of resonances as indicated in Table III. The 35-m results in each case are denoted by C, while the ANL results[5] are indicated by A. The isotopic identifications are all from Ref. 5.

Figure 3 shows examples of the area analysis for resonance parameters for a few arsenic levels, and Fig. 4 gives similar examples for some bromine levels.

III. DISCUSSION OF RESULTS

A. Mean Level Spacing and the Correlation Coefficients Between Adjacent Level Spacings

It is often quite difficult to decide whether a small rise in the cross section at some neutron energy is due to a weak resonance level or is due to a statistical fluctuation in the counts. In some cases, pure intuition is the deciding factor for omitting a "level" or including it as an "observed level." Moreover, an s- or p-wave assignment to such weak resonances is still more uncertain. Some alternative approach is thus desirable which can provide a better means of identifying such levels.

The subject of the statistical distribution of level spacings in complex nuclear spectra has been investigated by many authors during the last few

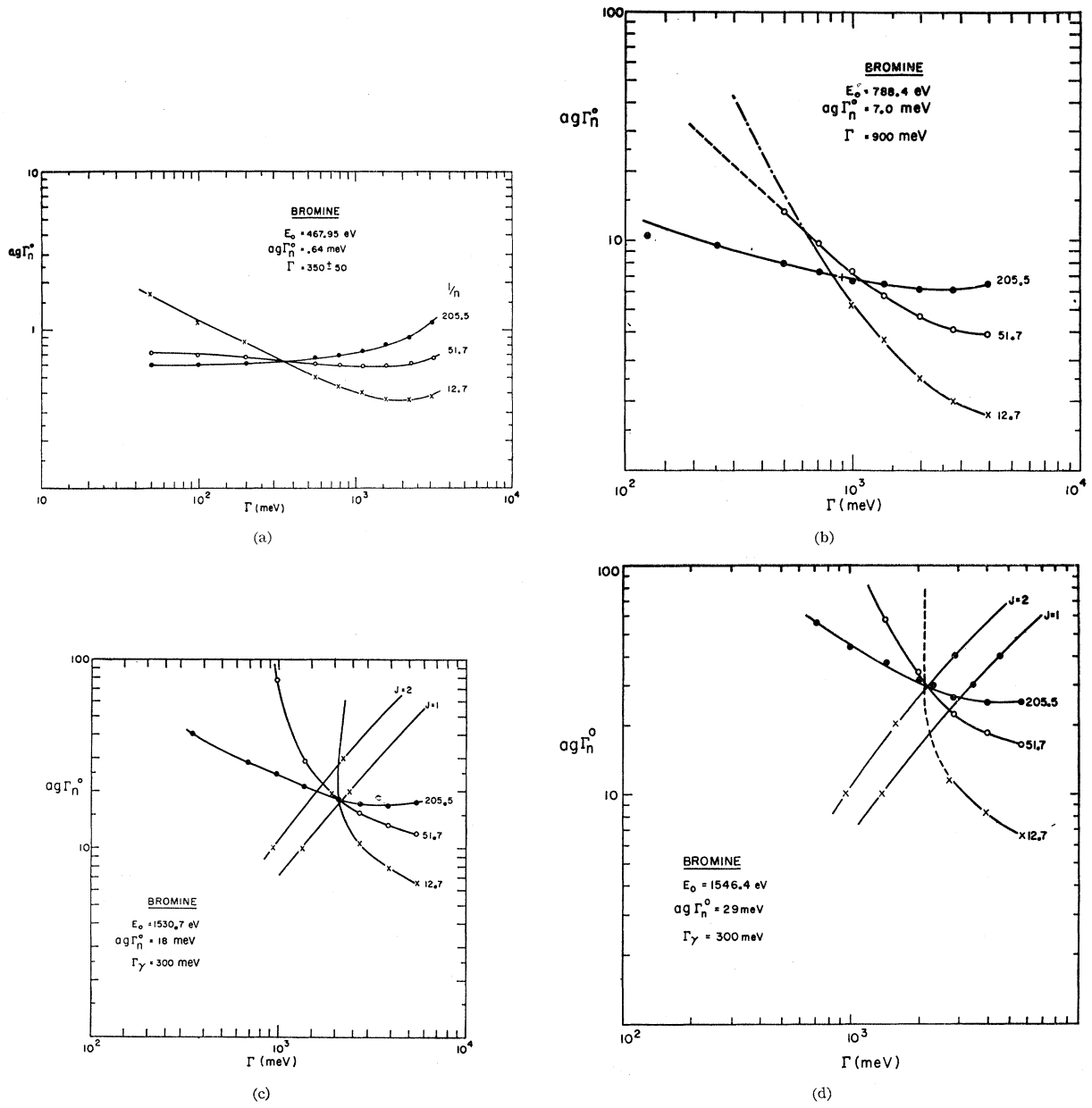

FIG. 4. Examples of the level parameter analysis for four levels in bromine. Refer to the caption of Fig. 3 for further comments.

years.[8–12] A summary of these theoretical developments has been given in the previous paper.[3] The present experimental data seem to provide fairly reasonable agreement with the theoretical predictions. One quantity of theoretical interest is the correlation coefficient between adjacent level spacings. Porter[9] has obtained a numerical value for this quantity of -0.253 for a single population using 3×3 matrices in an orthogonal ensemble. Calculations have been made by Leff[13] for cases involving more than one population and he obtains values close to that for a single population, although the reasoning is quite different when two merged populations are present. The reason why approximately the same large negative correlation coefficient between adjacent spacings is obtained for

[8] E. P. Wigner, Proceedings of the Gatlingburg Conference on Neutron Physics, ORNL Report No. 2309, 1957 (unpublished), p. 113.
[9] C. E. Porter and N. Rosenzweig, Suomalaisen Tiedeakat. Toimituksia, AVI44 (1960).
[10] F. J. Dyson, J. Math. Phys. 3, 140, 157, 166, 1199 (1962); F. J. Dyson and M. L. Mehta, *ibid.* 4, 701, 713 (1963).
[11] M. Gaudin, Nucl. Phys. 25, 447 (1961).
[12] P. B. Kahn, Nucl. Phys. 41, 159 (1963).
[13] H. Leff, University of Iowa, Report No. SUI63-23 (unpublished).

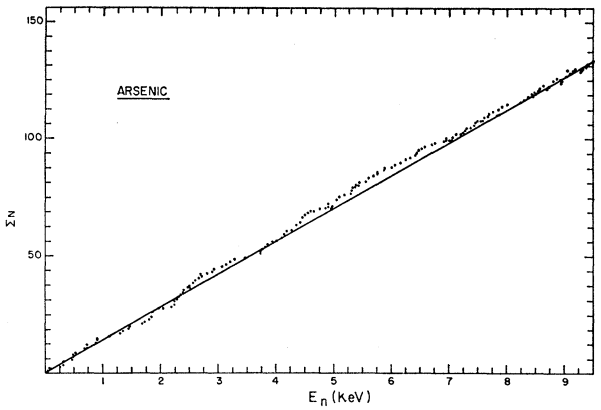

FIG. 5. The cumulative number of levels observed in As^{75} versus E_n.

two merged level populations as for a single population may occur as follows. Consider the case of two merged independent level sequences each having mean spacing $2\bar{D}$ for a net mean spacing $\bar{D}$. The Dyson theory[3] predicts a relatively crystalline spacing distribution for each sequence separately. Consider an extreme of a spacing distribution of exactly $2\bar{D}$ between members of each sequence, with a random relative positioning of the two sequences. If one spacing is D, then the adjacent spacing is $(2\bar{D}-D)$ and a small spacing is always adjacent to a larger spacing. A less extreme effect of this type could explain the theoretical result for two merged sequences.

In our preliminary investigation of these correlations in various nuclei[14] we found the correlation coefficient for some of the nuclei close to -0.20 ± 0.08. However, this value was very sensitive to the inclusion of certain levels. The effect was very striking for the case of U^{238}, where the correlation coefficient was almost zero when all "levels" were included. When a few of the very weak levels, whose $l=0$ nature was uncertain (p wave

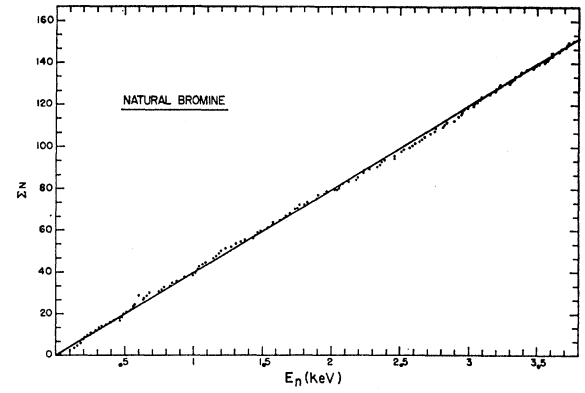

FIG. 6. The cumulative number of levels observed in Br versus E_n.

[14] J. B. Garg, Proceedings of the Symposium on the Statistical Properties of Complex Spectra, State University of New York, Stony Brook, Long Island, New York (unpublished).

or spurious), were excluded from the analysis a value of (-0.24 ± 0.07) was obtained in agreement with the theoretical value. Similar effects were observed in other nuclei as well. The change in the correlation coefficient was much smaller if a few strong levels were omitted. The effect on the correlation coefficient of the inclusion or omission of a very weak "level" has been found to be a useful auxiliary test for the retention or omission of doubtful $l=0$ resonances in our analysis. These resonances are marked with * in Tables I and II (starred levels) and were omitted from the subsequent statistical analyses. Even with these omissions the observed fractional number of weak levels is greater than expected for a Porter-Thomas distribution. It should be noted, of course, that when many weak levels are eliminated to make the resultant correlation coeffi-

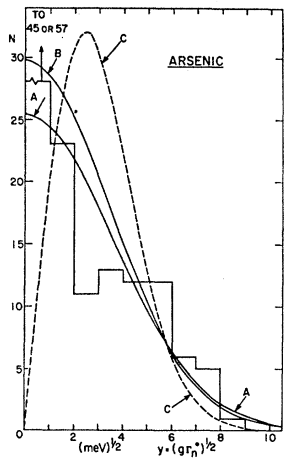

FIG. 7. A histogram of the observed experimental distribution of $y=[g\Gamma_n^0]^{1/2}$; for As^{75}. The theoretical curves are normalized to the observed $\Sigma(g\Gamma_n^0)$; strength function. Curves A and B are Porter-Thomas ($\nu=1$) theoretical distributions. Curve B is for 128 levels and $\langle g\Gamma_n^0\rangle=11.7$ meV. Curve A is for 115 levels and $\langle g\Gamma_n^0\rangle=13.1$ meV. Curve C corresponds to curve B, but is for $\nu=2$. It corresponds to an exponential distribution of $(g\Gamma_n^0)$ values. The values 57 and 45 for the first histogram interval correspond to the inclusion of all levels, and the omission of the starred levels (Table I), respectively.

cients have an *a priori* favored value, the subsequent significance of the value obtained for that correlation coefficient is correspondingly reduced.

A plot of the number of arsenic levels versus neutron energy is shown in Fig. 5 with the starred (uncertain) levels included. This plot shows a linear increase up to the maximum energy of 10 keV and suggests that relatively few $l=0$ levels have been missed in our measurements. A similar plot omitting starred levels has a slope corresponding to $\langle D\rangle=(75\pm5)$ eV. The indicated uncertainty is based partly on statistical considerations, but also reflects some uncertainty in the proper identification of $l=0$ resonances. The reasoning is similar to that previously given[3] for the cases of Th^{232} and U^{238}. An alternate analysis based only on the

strong levels is given in the next section and results in a slightly larger value for $\langle D\rangle$.

A similar plot of the number of levels versus neutron energy for the case of bromine is shown in the Fig. 6. This plot also shows an almost linear relationship up to the maximum energy investigated, thus indicating that practically all levels have been counted. A similar plot omitting starred levels has a slope corresponding to $\langle D\rangle=(27.4\pm1)$ eV. In this case also an analysis of the neutron width distribution based on the strong levels only leads to a slightly larger $\langle D\rangle$ value.

B. The Neutron Reduced Width Distributions and the $l=0$ Strength Functions

The distribution of the measured $g\Gamma_n^0$ values for arsenic was studied by dividing the data into two energy intervals: from 0–5000 eV and from 5000 to

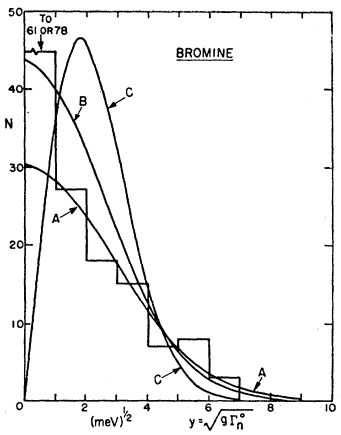

FIG. 8. A histogram of the observed distribution of $y=[g\Gamma_n^0]^{1/2}$; for natural bromine. The significance of the theoretical curves, and of the indicated positions for the first histogram box are the same as for Fig. 7. Curve A is for 110 levels and $\langle g\Gamma_n^0\rangle=8.46$ meV. Curves B and C are for 140 levels and $\langle g\Gamma_n^0\rangle=6.65$ meV.

10 000 eV. This was done to see if there was a gross difference in the width distribution for the upper and lower halves of the energy range where the energy resolution and other possible systematic effects might be different. Plots were made for both As and Br comparing the results for the upper and lower halves of the energy regions investigated after excluding starred "levels." No significant difference between the results for the two energy regions was noticed so the final plots presented here use all of the observed levels.

Figures 7 and 8 show the histograms of the number of values of $y=(g\Gamma_n^0)^{1/2}$ per unit $(\text{meV})^{1/2}$ for As and Br, respectively. In each case the vertical scale is chosen in such a way that the large number of cases for $y<1$ $(\text{meV})^{1/2}$ are not plotted directly, but the two indicated values in each case are for starred "levels" excluded, and for all "levels" included. The theoretical curves are of the "chi-squared" distribution[3] for $\nu=1$

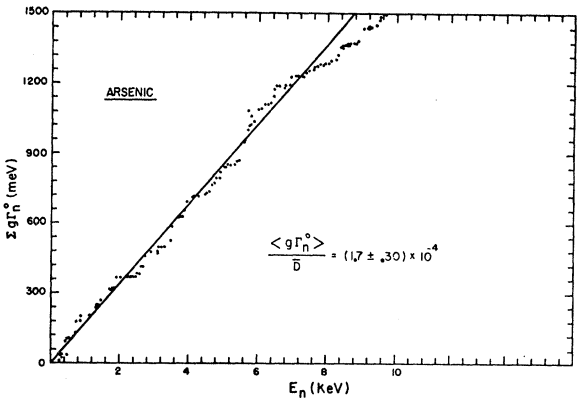

FIG. 9. $\Sigma(g\Gamma_n^0)$ versus E for As^{75}. The slope of the curve determines the $l=0$ strength function.

and 2

$$f(x)=\frac{\nu n x^{(\nu/2-1)}}{2\Gamma(\nu/2)}\exp[-\nu x/2],$$

where $\Gamma(\nu/2)$ is the gamma function, $x=y/\langle y\rangle$, and $\langle y\rangle n$ is the assumed number of levels for the theoretical curve. The $l=0$ strength function is based on $\sum g\Gamma_n^0$ for all levels and this sum is essentially independent of the number of very weak levels included. $\langle y^2\rangle$ is determined from this sum and the assumed number n of $l=0$ levels for the energy region studied. The value of n depends on the number of very weak "levels" which are treated as spurious or belonging to a different population. The $\nu=1$ curve is the Porter-Thomas shape while the $\nu=2$ curve, for two channels, corresponds to an exponential distribution for $g\Gamma_n^0$ values. In each case curve B is the Porter-Thomas distribution normalized to the number of levels observed when "starred levels" are excluded. Curve A is the Porter-Thomas distribution normalized for a smaller number of levels which gives a better fit to the portion of the histogram $y>1$. Curve C is the $\nu=2$ curve corresponding to curve B. For As, curves B and C are for 128 levels

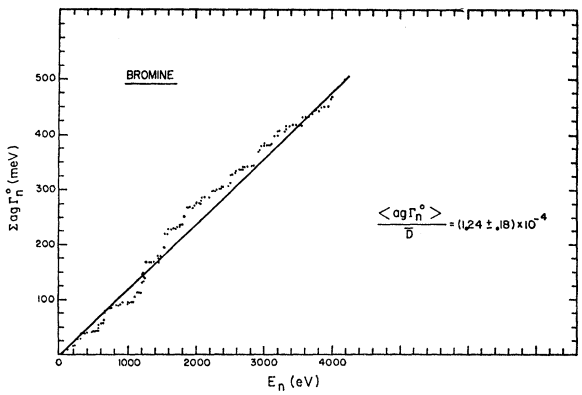

FIG. 10. $\Sigma(ag\Gamma_n^0)$ versus E for natural bromine. The slope of the curve determines the average of the strength functions for Br^{79} and Br^{81}. Each isotope has $a=0.50$.

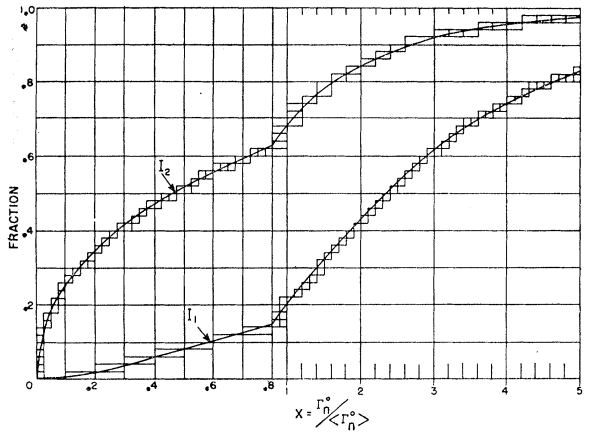

FIG. 11. Theoretical curves of distribution parameters for a single population Porter-Thomas ($\nu=1$) distribution of reduced neutron widths. I_1 is the fraction of $\Sigma\, g\Gamma_n^0$ expected for $x \equiv g\Gamma_n^0/\langle g\Gamma_n^0\rangle$ less than the value of the abscissa. Similarly, I_2 is the fraction of the levels having the given x or smaller.

$\langle g\Gamma_n^0\rangle = 11.7$ meV, while the Porter-Thomas best fitting curve A is for $n=115$ levels, $\langle g\Gamma_n^0\rangle = 13.1$ meV, and $\langle D\rangle = 87$ eV.

For Br, curves B and C of Fig. 8 are for $n=140$ and $\langle g\Gamma_n^0\rangle = 6.65$ meV. Curve A is for $n=110$, $\langle g\Gamma_n^0\rangle = 8.46$ meV, and gives $\langle D\rangle = 36.5$ eV.

Figures 9 and 10 show the plots of $\sum g\Gamma_n^0$, for As, and $\sum ag\Gamma_n^0$ for Br versus energy. The average slope of these plots determine the $l=0$ strength functions S_0 for As and Br. In the case of As the S_0 value is the weighted average for the $J=1$ and $J=2$ spin states. In the case of Br, it is the isotopic average, giving equal weightings to Br^{79} and Br^{81}, and is also the weighted average of the $J=1$ and $J=2$ states for both isotopes.

As was also observed for the cases of Th^{232} and U^{238}, the strength function values seem to decrease gradually towards the high-energy end. This might suggest that there may be systematic experimental effects which give slightly low S_0 values at the higher energies.

TABLE IV. Neutron ($g\Gamma_n^0$) distribution for arsenic.[a]

Energy interval (eV)	No. of levels	Mean $\langle g\Gamma_n^0\rangle$ (meV)	ν^a	$\frac{1}{n}\Sigma \mathrm{n}\frac{g\Gamma_n^0}{\langle g\Gamma_n^0\rangle}$	ν^b
(omitting starred levels)					
0–2000	23	15.83	1.34	−1.15	1.10±0.27
0–4000	52	13.68	1.16	−1.59	0.84±0.13
0–6000	82	13.36	1.14	−1.49	0.87±0.11
0–8000	107	12.05	1.08	−1.53	0.86±0.10
0–9700	128	11.71	1.08	−1.40	0.93±0.09
(including all "levels")					
0–2000	25	14.57	1.17	−1.45	0.88±0.20
0–4000	57	12.49	1.00	−1.89	0.73±0.11
0–6000	88	12.45	1.03	−1.78	0.76±0.10
0–8000	114	11.31	0.98	−1.76	0.77±0.09
0–9700	136	11.03	0.98	−1.56	0.85±0.09

[a] The quantity ν^a is based on the fractional dispersion of the distribution as suggested by Wilets, while ν^b is based on a maximum likelihood method proposed by Porter and Thomas.

TABLE V. Neutron ($g\Gamma_n^0$) distribution for bromine.[a]

Energy interval (eV)	Number of levels	(meV) $\langle ag\Gamma_n^0\rangle$	ν^a	$\frac{1}{n}\Sigma \ln\left(\frac{g\Gamma_n^0}{\langle g\Gamma_n^0\rangle}\right)$	ν^b	$\Delta\nu^b$
(omitting starred levels)						
0–1000	35	5.34	0.97	−1.40	0.93	0.18
0–2000	70	7.66	0.86	−1.48	0.88	0.11
0–3000	105	7.20	0.90	−1.51	0.87	0.10
0–4000	141	6.40	0.81	−1.64	0.81	0.09
(including all "levels")						
0–1000	39	4.80	0.83	−1.69	0.79	0.15
0–2000	78	6.76	0.72	−1.77	0.77	0.11
0–3000	117	6.38	0.77	−1.77	0.77	0.08
0–4000	156	5.78	0.71	−1.85	0.74	0.07

[a] See note on Table IV.

The "preferred" S_0 values thus give slightly greater weightings to the lower 80% of the energy range and we choose

$$S_0 = (1.70\pm0.30)\times10^{-4} \text{ for arsenic,}$$
$$S_0 = (1.20\pm0.18)\times10^{-4} \text{ for bromine.}$$

The quoted uncertainties are larger than those required from statistical considerations based on the number of levels involved in order to take account of possible systematic errors.

The distribution of $g\Gamma_n^0$ would be expected to follow the Porter-Thomas distribution for a single population (i.e., a single isotope and spin state $l=0$ levels, where all levels are from an ensemble having a common ($\langle\Gamma_n^0\rangle$). When levels of two spin values are present for a single isotope the $\langle g\Gamma_n^0\rangle$ values for the two spin states could be equal. The required condition is the equality of the two products, $(gS_0\langle D\rangle)$ for the two different J values. In the case where more than one isotope is also present, as for Br, the product $(agS_0\langle D\rangle)$ must be the same for all isotope and J values to have a common $\langle ag\Gamma_n^0\rangle$. Since $a=\frac{1}{2}$ and $I=\frac{3}{2}$ for both isotopes, the factor a may be omitted and $g\Gamma_n^0$ used in the preceding discussion.

In terms of an optical model we know of no good reason why Br^{79} and Br^{81} should be expected to have very different values for S_0 or for their level densities. A simple statistical model approach[15] suggests that the level density for a given J, $\rho_J = [\langle D_J\rangle]^{-1}$, should be proportional to $(2J+1)$ times a Gaussian factor which reduces to ρ_J for large J. In Table I, including the uncertain J values assignments, 16 levels are denoted $J=2$ and 7 levels are denoted $J=1$. This gives a somewhat greater ratio of $J=2$ to $J=1$ levels than the ratio 5 to 3 expected from the $(2J+1)$ values. Table III indicates for Br that there are 2 levels where $J=1$ is favored and 7 levels where $J=2$ is favored. References to neutron cross-section compendia[16] shows that, to the extent that the resonance level angular momenta

[15] C. Bloch, Phys. Rev. **93**, 1094 (1954).
[16] D. J. Hughes, B. A. Magurno, and M. K. Brussel, Supplement Number 1 to BNL-325, 2nd ed. (January 1960).

TABLE VI. Correlation coefficients for arsenic and bromine, between adjacent level $g\Gamma_n^0$ values, and between the $g\Gamma_n^0$ values for a level and the average of its two level spacings from its adjacent levels.

Energy interval (eV) and element	$\rho[g\Gamma_n{}^0{}_{-j} - g\Gamma_n{}^0{}_{(j+1)}]$ All levels		$\rho[g\Gamma_n{}^0{}_{-j} - g\Gamma_n{}^0{}_{(j+1)}]$ Less * levels		$\rho\left[g\Gamma_n{}^0{}_j - \left(\frac{E_{j+1}-E_{j-1}}{2}\right)\right]$ All levels		$\rho\left[g\Gamma_n{}^0{}_j - \left(\frac{E_{j+1}-E_{j-1}}{2}\right)\right]$ Less * levels	
	ρ	$\Delta\rho$	ρ	$\Delta\rho$	ρ	$\Delta\rho$	ρ	$\Delta\rho$
				Arsenic				
0–1000	−0.22	0.27	−0.15	0.26	0.04	0.30	0.13	0.27
0–2000	−0.35	0.19	−0.30	0.18	0.12	0.22	0.16	0.20
0–4000	−0.02	0.14	0.03	0.13	0.29	0.13	0.36	0.11
0–6000	0.06	0.11	0.09	0.11	0.28	0.11	0.33	0.10
0–8000	0.06	0.10	0.08	0.09	0.22	0.09	0.26	0.09
0–9700	0.06	0.09	0.06	0.08	0.24	0.08	0.26	0.08
Weighted mean	0.06	0.09	0.06	0.09	0.24	0.08	0.26	0.08
				Bromine				
0–1000	−0.07	0.16	−0.11	0.17	0.02	0.16	−0.06	0.17
0–2000	0.16	0.11	0.25	0.11	0.05	0.11	0.10	0.12
0–3000	0.14	0.09	0.22	0.09	−0.02	0.09	0.04	0.10
0–4000	0.11	0.08	0.19	0.08	−0.01	0.08	0.07	0.08
Weighted mean	0.12	0.08	0.20	0.08	−0.01	0.08	0.06	0.09

have been assigned for odd-A nuclei (Hg, Pt^{195}, W^{185}, Cd^{113}) there are considerably more than twice as many assignments for $J=I+\frac{1}{2}$ than for $J=I-\frac{1}{2}$. W^{183} is an exception where five $J=1$ values and four $J=0$ values are listed. This general unexpectedly large fraction of the cases where the spin assignment is to the larger of the two possible J values is interesting, but a greater sampling of high reliability results is required before definite conclusions can be made. There is always the misgiving that there is an experimental bias which tends to favor assignment to high J states.

If one assumes that the intrinsic optical-model strength function S_0 is the same for $(I+\frac{1}{2})$ and $(I-\frac{1}{2})$ states, then $\langle(\Gamma_n^0)_J\rangle$ should be proportional to $\langle D_J\rangle$. If ρ_J is proportional to $(2J+1)$, then $\langle(\Gamma_n^0)_J\rangle$ should vary with J as $g_J{}^{-1}$, and $\langle(g\Gamma_n^0)_J\rangle$ should be the same for the two J states and should act as if they belonged to the same population when the distribution of $\langle g\Gamma_n^0\rangle$ values is considered. If the above assumptions do not apply, the experimental distribution of widths should give a better fit for $\nu<1$.

Best values of ν for the neutron width distribution were determined for As and Br using each of the two methods described in the preceding paper[3] for Th^{232} and U^{238}. The quantity ν^a is based on the fractional dispersion of the distribution as suggested by Wilets, while ν^b is based on a maximum likelihood method proposed by Porter and Thomas. In Tables IV and V the results are given for ν^a and ν^b for As and Br for the starred "levels" excluded, and for all "levels" included for different cumulative energy intervals.

Both the best fit ν^a and ν^b values, are less than unity in view of the large excess of weak levels (Figs. 7 and 8). Hence ν is closer to unity when the starred "levels" are omitted from the analysis. Most of the excess weak levels probably have $l=1$. However, we cannot say which of these weak levels have $l=0$ and which have $l=1$.

A rough analysis was used to obtain a best "Porter-Thomas" fit to the results using only the stronger levels, which give the main contribution to the strength function. Figure 11 shows the values I_1 and I_2 for a Porter-Thomas distribution of neutron reduced widths. I_1 is the fraction of $\sum g\Gamma_n^0$ expected for $x\equiv g\Gamma_n^0/\langle g\Gamma_n^0\rangle$ less than the value of the abscissa. Similarly I_2 is the fraction of the levels having the given x or smaller.

The method of using these curves for As and Br was as follows. The experimental $g\Gamma_n^0$ values were first arranged in order of increasing magnitude. Cumulative sums of the $g\Gamma_n^0$ values were then obtained starting from the smallest value of $g\Gamma_n^0$ and ending with the given $g\Gamma_n^0$ value in the listing (partial sum). The sum of the $g\Gamma_n^0$ values for all levels was also obtained (total sum). Dividing each partial sum by the total sum we obtained a fractional sum value for each $g\Gamma_n^0$ value. For various choices of $g\Gamma_n^0$ the value of the fractional sum defined an ordinate value on curve I_1 of Fig. 11. The corresponding abscissa value defined the value of x to be associated with the given $g\Gamma_n^0$ value. Values of $\langle g\Gamma_n^0\equiv g\Gamma_n^0/x$ and $n\equiv\sum g\Gamma_n^0/\langle g\Gamma_n^0\rangle$ were then established for various choices of $g\Gamma_n^0$. The choice of $g\Gamma_n^0$ in the range from 24 to 33 meV for As suggested $n\approx 115$ and $\langle g\Gamma_n^0\rangle\approx 13.1$ meV. For Br it was similarly found that values of $g\Gamma_n^0$ having about 50% of the strength function for those or smaller values of $g\Gamma_n^0$ implied that $n\approx 111$ and $\langle g\Gamma_n^0\rangle\approx 8.35$ meV. These are essentially the parameters for curves A of Figs. 7 and 8. This method is probably of very low precision due to the small number of levels involved, but the resulting A curves of Figs. 7 and 8 give a fairly good fit to the data for all but the weakest levels.

Most of the strong levels of As up to 4 keV have

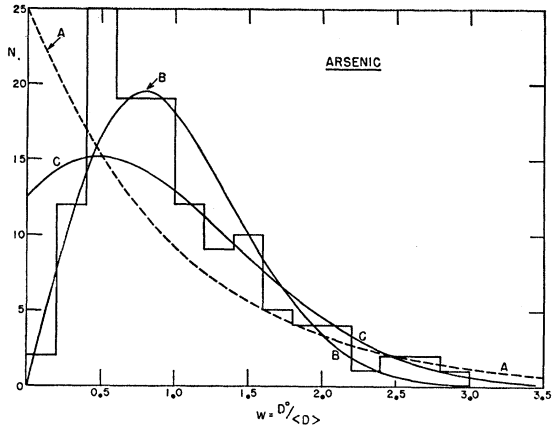

FIG. 12. Histogram of the observed distribution of nearest-neighbor level spacings $w=D^0/\langle D\rangle$ for As^{75} when starred levels (Table I) are omitted. Curve A, for a random occurrence of levels, corresponds to a simple exponential spacing distribution for w. Curve B is the single population Wigner (orthogonal) distribution. Curve C is for two randomly positioned Wigner distributions for the case of equal $\langle D\rangle$ for the separate populations.

been assigned J values subject to the above reservations. Separate values of S_0 for the $J=2$ and $J=1$ levels for arsenic can be given as $(2.4\pm0.9)\times10^{-4}$ for $J=2$, $(0.8\pm0.4)\times10^{-4}$ for $J=1$.

C. Other Correlation Coefficients

The correlation coefficients $\rho(g\Gamma_{n-j}{}^0-g\Gamma_n{}^0{}_{(j+1)})$ between the $g\Gamma_n{}^0$ values of adjacent levels has been investigated for various cumulative energy intervals for As and Br. The correlation coefficient, $\rho\{g\Gamma_n{}^0{}_j-[(E_{j+1}-E_{j-1})/2]\}$ between the $g\Gamma_n{}^0$ value for a level, and the average of its two level spacings with respect to adjacent levels, was also tested. The results of both tests for As and Br are given in Table VI. We know of no convincing theoretical arguments that these parameters should be different from zero and it may even prove to be a test of experimental bias if the results are significantly different from zero. However, an examination of the experimental situations seems to be warranted.

The small net positive width-width correlation for As and Br seems to be consistent with zero. As discussed previously,[3] the greater likelihood of missing a weak level adjacent to a strong level would lead to an expected small bias towards a positive correlation coefficient. The initial negative values for the low-energy region for As could be caused by a statistical fluctuation.

The width-spacing correlation for Br is essentially zero, but the As values are rather large to be consistent with zero. In the discussion[3] of the Th^{232} and U^{238} results, we noted that experimental bias favors missing a weak level near to adjacent resonances. This bias also applies for the As and Br results.

D. Nearest-Neighbor Level Spacing Distributions

Figures 12 and 13 show the distribution of nearest-neighbor level spacings for arsenic and bromine, respectively. In both cases the starred levels in Tables I and II were excluded. In each case three theoretical[2,3] curves are shown. Curve A, for a random occurrence of levels, corresponds to a simple exponential spacing distribution for $w=D^0/\langle D\rangle$. The single population orthogonal distribution, curve B, should not apply exactly, since there are two merged $l=0$ spin populations for As and four for Br, counting the two isotopes and two spin states. Moreover, if various $l=1$ populations are also included, the curve should be closer to that expected from a random distribution. Curve C corresponds to two mixed orthogonal populations[2] for the case of equal $\langle D\rangle$ for the separate populations. The term "orthogonal" refers to Dyson's "threefold-way" distribution[3] of the orthogonal, unitary, and sympletic ensembles.

For both arsenic and bromine the best fit seems to be obtained for the single-orthogonal case. For arsenic this could be explained because the $J=2$ states are considerably more numerous than the $J=1$ states. For bromine the result is harder to understand, since there are two isotopes. The isotope assignment in Table III lists 8 levels for Br^{79}, but only 3 levels for Br^{81}. These data would be more convincing in suggesting that $\langle D\rangle$ is much larger for Br^{81} than for Br^{79} if it were not for the fact that the three Br^{81} levels occupy a region of about 100 eV, while the Br^{79} levels occupy a region of about 400 eV. Table VII shows the results of a χ^2 test of the experimental level spacing distributions using the theoretical (1) random distribution, (2) single orthogonal distribution, and (3) two equal spacing merged orthogonal populations. The first four moments M^1 to M^4 of the experimental distribution are also given, along with the theoretical value for a single orthogonal ensemble. The spacing distribution results

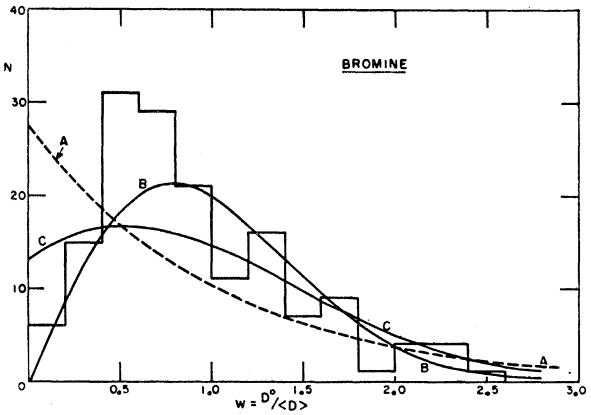

FIG. 13. Histogram of the observed distribution of nearest-neighbor level spacings for natural Br. The theoretical curves have the same significance as in Fig. 12.

TABLE VII. Modified χ^2-tests and moments M^k for the nearest-neighbor spacing distribution for arsenic and bromine.

Nucleus	Energy region (eV)	No. of levels considered	$\langle D\rangle$ (eV)	χ^2-values $P_R{}^0$	$P_0{}^0(1)$	$P_0{}^0(2)$	Moments-M^k M^1	M^2	M^3	M^4
As	0–4850	64	75.5	20.7	9.31	11.64	1.00	1.40	2.45	4.90
As	0–9700	128	75.5	43.5	12.7	21.40	1.00	1.35	2.28	4.46
As	4850–9700	64	75.5	26.0	5.9	12.7	1.00	1.31	2.10	3.86
Br	0–2000	71	28.2	28.6	15.4	15.7	1.00	1.40	2.42	4.77
Br	0–4000	140	28.6	48.8	27.7	25.8	1.00	1.38	2.38	4.60
Br	2000–4000	69	29.0	24.7	15.7	16.2	1.00	1.39	2.40	4.70
Theory (Porter)	10×10 matrices (single population)						1.00	1.32	2.12	3.93

for the upper half of the energy range should be the least reliable in each case, so separate calculations are made using the first half, and using the entire energy range. Any experimental bias would be in the direction of missing small level spacings. This bias would, in fact, tend to give a better fit to the single population theoretical distribution in agreement with our observations. The results in Table VII show that the single orthogonal case is strongly favored for both As and Br, particularly when the full energy range is included.

E. Next-Nearest-Neighbor Spacing Distributions

Figures 14 and 15 show the distribution of the next-nearest-neighbor level spacings D^1 for arsenic and bromine in terms of $w=D^1/\langle D^0\rangle$, where $\langle D^0\rangle$ is the average of the single spacings. This means that $\langle w\rangle=2$. The three curves shown are all theoretical[3] next-nearest-neighbor spacing distributions. Curve A is for the random case distribution of energy levels. Curve B, due to Porter and Kahn, is for a single population orthogonal ensemble. Curve C, due to Leff,[13] is an extension of the Porter-Kahn results for the case of two merged level sequences of equal density.

The results of the χ^2 tests are shown in Table VIII. As in Table VII, the first four moments of the spacing distribution are also shown. These moments would be

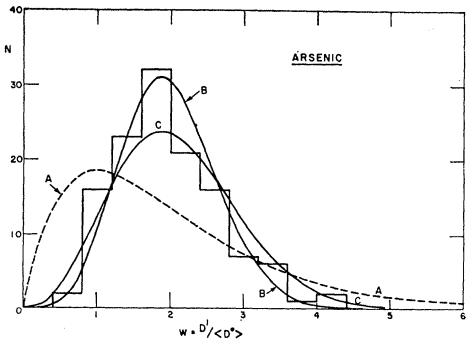

FIG. 14. Histogram of the observed distribution of next-nearest-neighbor level spacings $w=D^1/\langle D^0\rangle$ for As[75]. The three curves are all theoretical next-nearest-neighbor curves. Curve A is the random case. Curve B, due to Porter and Kahn, is for a single population orthogonal ensemble. Curve C, due to Leff, is for two merged orthogonal level sequences of equal density.

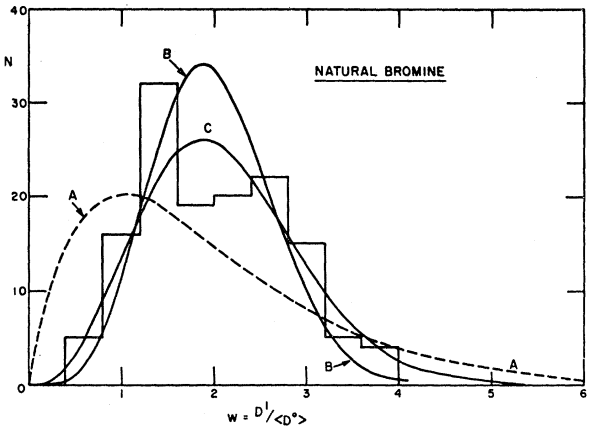

FIG. 15. Histogram of the observed distribution of next-nearest-neighbor level spacings $w=D^1/\langle D^0\rangle$ for natural Br. The theoretical curves have the same meaning as in Fig. 14.

2, 4, 8, 16 for a constant level spacing distribution. The last column gives the predicted result corresponding to the Porter-Kahn curves in Figs. 13 and 14. The column $P_0{}^{(4)}$ for Br refers to Leff's results[13] for four equal density merged orthogonal ensembles. The theoretical values of the moments are Monte Carlo calculation results using 10×10 matrices.[3] A comparison was also made with the case of a single unitary ensemble. The results are not included, but large χ^2 values were obtained. The χ^2 values show comparable agreement for $P_0{}^1(1)$ and $P_1{}^1(2)$ for arsenic. For bromine the agreement with $P_0{}^1(2)$ is best. In both cases the fit is quite poor for the random case. The comments of the preceding section should be noted in connection with these results.

F. Correlation Between Level Spacings

The correlation coefficients for adjacent level spacings for arsenic and bromine are given in Table IX using various cumulative energy intervals. In both cases, the correlation coefficient including all levels is about (-0.08 ± 0.08), while the values are $-(0.20\pm0.08)$ for arsenic and $-(0.24\pm0.08)$ for bromine when the starred levels in Tables I and II are omitted. The theoretical value for two equal density merged orthog-

TABLE VIII. Modified χ^2-tests and moments M^k for the next-nearest neighbor spacing distribution for arsenic and bromine.

Nucleus	Energy region (eV)	No. of levels considered	$\langle D\rangle$ (eV)	χ^2 values $P_R{}^1$	$P_0{}^1(1)$	$P_0{}^1(2)$	$P_0{}^1(4)$	Moments M^k M^1	M^2	M^3	M^4
As	0–4850	64	75.5	31.9	16.9	15.0	19.1	2.00	4.54	11.80	34.7
As	0–9700	128	75.5	73.1	19.1	22.6	37.9	2.00	4.52	11.60	33.4
As	4850–9700	64	75.5	46.4	14.0	18.5	27.6	2.00	4.50	11.2	31.4
Br	0–2000	71	28.2	44.9	29.4	22.7	27.1	2.00	4.66	12.0	33.4
Br	0–4000	140	28.6	62.7	30.9	19.2	28.7	2.00	4.56	11.7	32.4
Br	2000–4000	69	29.0	32.6	15.9	13.8	18.2	2.00	4.53	11.5	32.4
Theory (Porter)	10×10 matrices (single population)							2.00	4.48	11.1	29.9

TABLE IX. Adjacent level spacing correlations as a function of neutron energy for arsenic and bromine.

Energy interval (eV)	Arsenic: All levels included	Arsenic: Levels marked with * excluded
0–2000	−0.16±0.20	−0.30±0.20
0–4000	−0.13±0.13	−0.27±0.13
0–6000	−0.11±0.11	−0.24±0.10
0–8000	−0.08±0.10	−0.23±0.09
0–9700	−0.07±0.09	−0.20±0.08
Mean cumulative	−0.07±0.09	−0.20±0.08

Energy interval (eV)	Bromine: All levels included	Bromine: Uncertain levels excluded from the analysis
0–1000	−0.01±0.16	−0.26±0.16
0–2000	−0.02±0.11	−0.20±0.12
0–3000	−0.09±0.09	−0.26±0.09
0–4000	−0.08±0.08	−0.22±0.08
Weighted mean	−0.08±0.08	−0.24±0.08

onal ensembles is $-(0.26\pm0.03)$ on the basis of random matrix calculations. As pointed out earlier, the significance of the agreement is somewhat diminished because the choice of assigning an asterisk to a level was partly based on the effect of its omission on this parameter.

Table X shows the higher order correlation coefficients ρ^k for k spacings between a given pair of spacings. The results for $k\geqslant 1$ are probably all consistent with zero.

TABLE X. Higher order level spacing correlations for arsenic and bromine. ρ^k is the correlation coefficient for level spacings having k intermediate spacings. The "theoretical" results are the results of random matrix calculations for two equal merged orthogonal ensembles. The levels indicated by * in Tables I and II are not included. Upper energy limits of 8 keV and 3 keV were for As and Br, respectively.

k	Arsenic ρ^k	Arsenic $\Delta\rho^k$	Bromine ρ^k	Bromine $\Delta\rho^k$	Theoretical ρ^k	Theoretical $\Delta\rho^k$
0	−0.23	0.09	−0.25	0.09	−0.26	0.03
1	0.18	0.10	−0.08	0.09	−0.08	0.03
2	0.01	0.10	−0.11	0.09	−0.05	0.03
3	−0.05	0.10	0.13	0.09	+0.01	0.03

CONCLUSION

The experimental results for the statistical properties of levels obtained in the high resolution neutron total cross-section measurements of arsenic and natural bromine have been compared with various theoretical predictions of the random matrix model initially suggested by Wigner and further developed by Porter and others. The general agreement of the present data with the theory is good except for a few discrepancies. Among these are fewer small spacings and more small $g\Gamma_n{}^0$ values observed than the theoretical distributions predict. The observance of fewer small level spacings than expected is probably due to experimental difficulties and the excess of small $g\Gamma_n{}^0$ values is probably due to p-wave levels.

Another important result is the apparent dependence of the $l=0$ strength function, $S_0\equiv\langle g\Gamma_n{}^0\rangle/\langle D\rangle$, on the value of J for the compound nucleus. Levels having $J=(I+\frac{1}{2})$, for arsenic and bromine, seem to have a much larger strength function than levels having $J=(I-\frac{1}{2})$.

The values of the s-wave strength function S_0 for arsenic averaged over spin states is $(1.70\pm0.30)\times10^{-4}$ and for bromine averaged over isotopes and spin states is $(1.20\pm0.18)\times10^{-4}$. These results are consistent with the variation of S_0 with atomic mass expected from calculations using the optical model when account is taken of the extent to which freedom of choice remains in the values of theoretical parameters used to fit the over-all body of experimental results.

ACKNOWLEDGMENTS

The authors take great pleasure in acknowledging the assistance of Dr. J. S. Petersen and velocity selector technicians, A. Blake, S. Marshall, J. Spiteri, and D. Ryan in the various phases of these measurements. Bum-Nai Ham and Young-Hee Ham were very helpful in the final analysis of the data. Useful discussions with Dr. C. E. Porter and Dr. P. B. Kahn are gratefully acknowledged. Dr. J. L. Rosen and Dr. J. S. Desjardins made major contributions to the 1959–1960 self-indication measurements for As and Br using a 35-m flight path. Finally, we wish to express our appreciation for the assistance rendered by the technical staff of the Nevis synchrocyclotron.

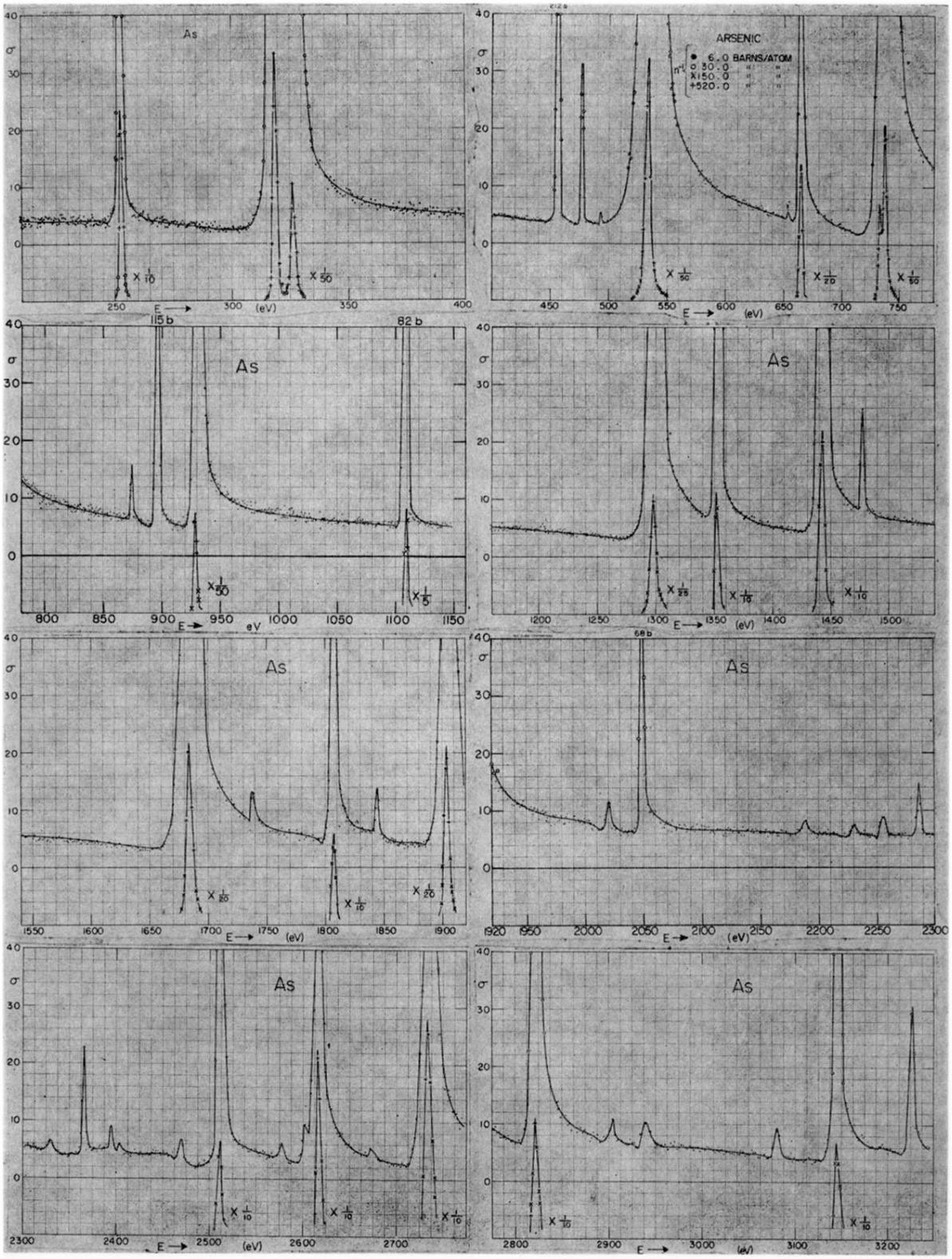

(a)

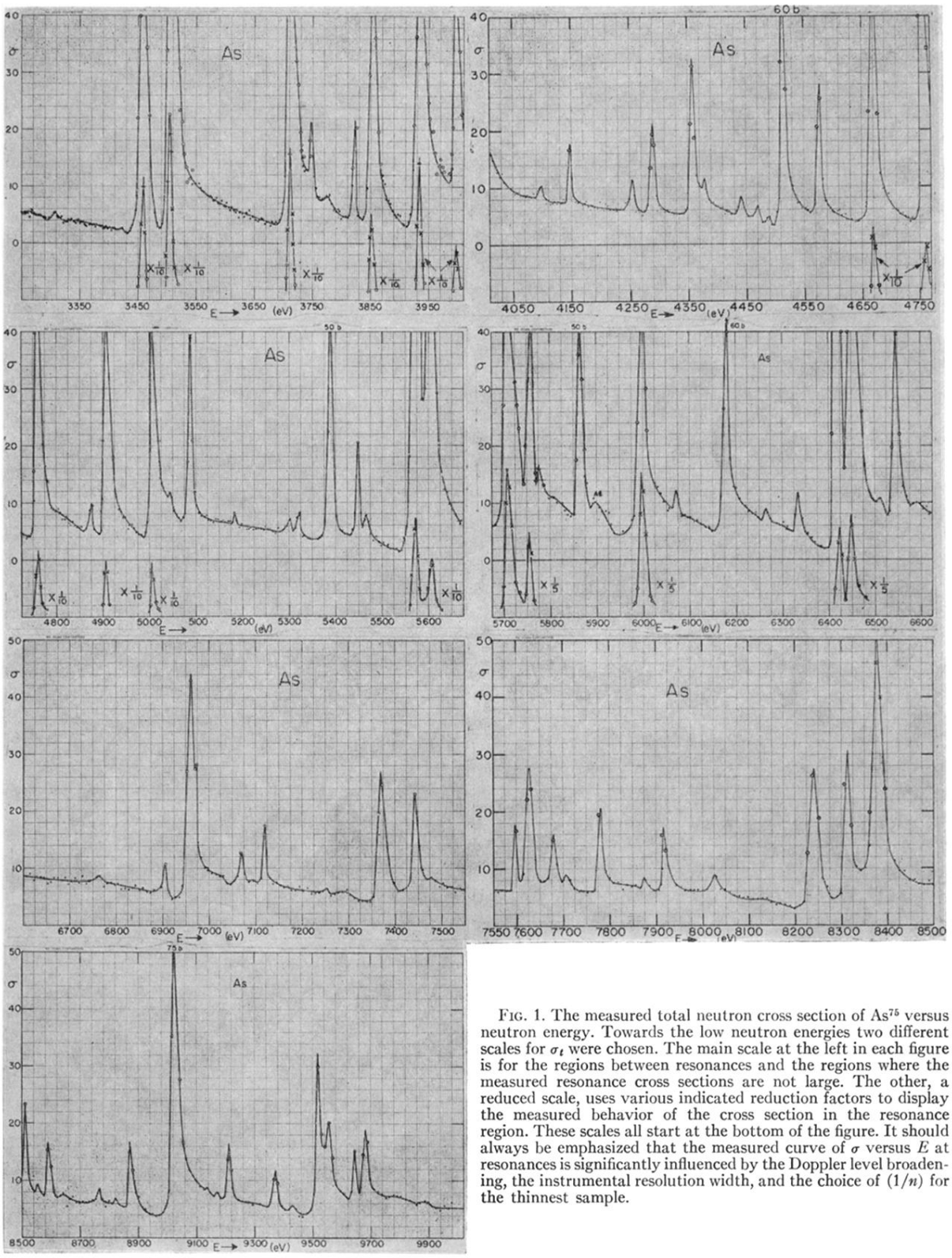

FIG. 1. The measured total neutron cross section of As^{75} versus neutron energy. Towards the low neutron energies two different scales for σ_t were chosen. The main scale at the left in each figure is for the regions between resonances and the regions where the measured resonance cross sections are not large. The other, a reduced scale, uses various indicated reduction factors to display the measured behavior of the cross section in the resonance region. These scales all start at the bottom of the figure. It should always be emphasized that the measured curve of σ versus E at resonances is significantly influenced by the Doppler level broadening, the instrumental resolution width, and the choice of $(1/n)$ for the thinnest sample.

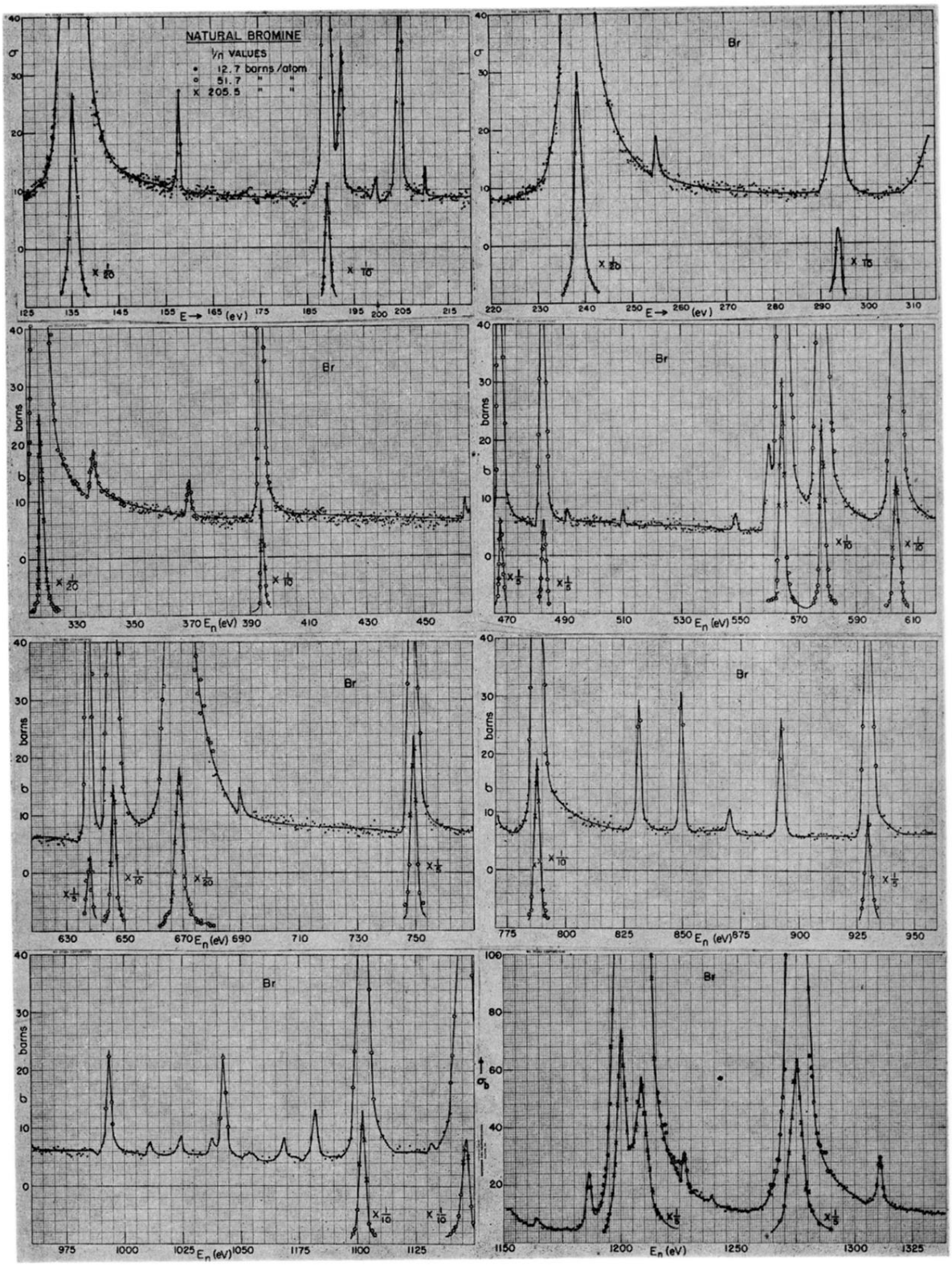
NATURAL BROMINE
1/n VALUES
• 12.7 barns/atom
○ 51.7 " "
X 205.5 " "
Br
σ
barns
E → (eV)
E_n (eV)

(a)

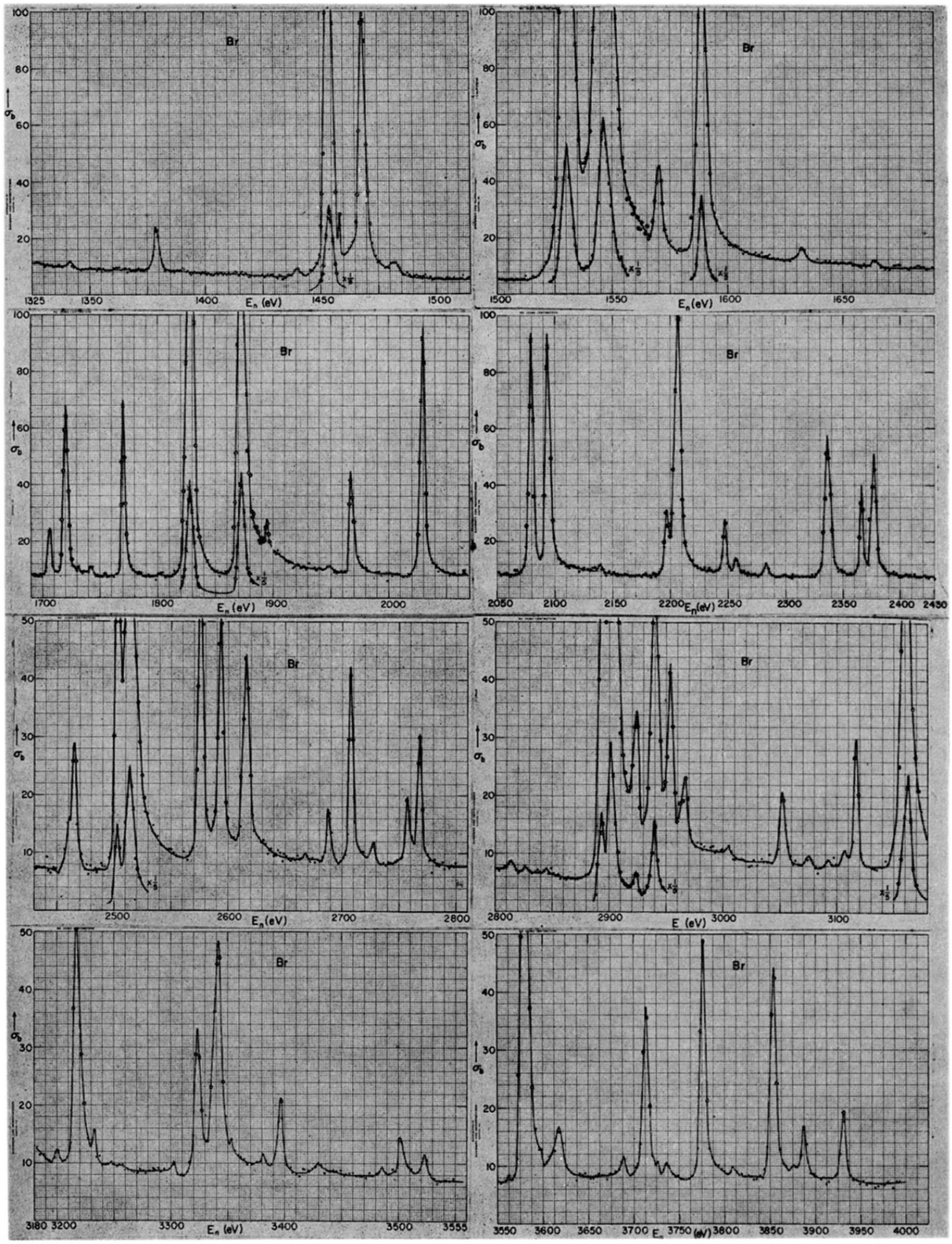

(b)

FIG. 2. The "measured" cross section of Br versus neutron energy. Values are for the natural element which has about 50% abundance each of Br^{79} and Br^{81}. The "measured" peak cross sections are limited experimentally to values which are not large compared to the value $(1/n) = 205.5$ b/atom of the thinnest sample, so they may be small compared with the true Doppler-broadened peak cross section.